



**INVESTIGATION OF THE EFFECT OF BLAST
FURNACE SLAG, GLASS POWDER AND
METAKAOLIN ADDITIONS ON THE ALKALINE
ACTIVATION OF KAOLINITE**

**2021
MASTER'S THESIS
METALLURGY AND MATERIALS ENGINEERING**

ZAID MOHAMMED ALI KAREEM KAREEM

**Thesis Advisor
Dr. Süleyman YAŞIN**

**INVESTIGATION OF THE EFFECT OF BLAST FURNACE SLAG, GLASS
POWDER AND METAKAOLIN ADDITIONS ON THE ALKALINE
ACTIVATION OF KAOLINITE**

Zaid Mohammed Ali Kareem KAREEM

T.C.

Karabuk University

Institute of Graduate Programs

Department of Metallurgy and Materials Engineering

Prepared as

Master Thesis

Thesis Advisor

Dr. Süleyman YAŞIN

KARABUK

May 2021

I certify that in my opinion the thesis submitted by Zaid Mohammed Ali Kareem KAREEM titled “INVESTIGATION OF THE EFFECT OF BLAST FURNACE SLAG, GLASS POWDER AND METAKAOLIN ADDITIONS ON THE ALKALINE ACTIVATION OF KAOLINITE” is fully adequate in scope and in quality as a thesis for the degree of Master of Science.

Dr. Süleyman YAŞIN
Thesis Advisor, Department of Metallurgy and Materials Engineering

This thesis is accepted by the examining committee with a unanimous vote in the Department of Metallurgy and Materials Engineering as a Master of Science thesis.
31.05.2021

<u>Examining Committee Members (Institutions)</u>	<u>Signature</u>
Chairman : Dr. Yüksel AKINAY (YYU)
Member : Dr. Engin ÇEVİK (KBU)
Member : Dr. Süleyman YAŞIN (KBU)

The degree of Master of Science by the thesis submitted is approved by the Administrative Board of the Institute of Graduate Programs, Karabuk University.

Prof. Dr. Hasan SOLMAZ
Director of the Institute of Graduate Programs

“I declare that all the information within this thesis has been gathered and presented in accordance with academic regulations and ethical principles and I have according to the requirements of these regulations and principles cited all those which do not originate in this work as well.”

Zaid Mohammed Ali Kareem KAREEM

ABSTRACT

M. Sc. Thesis

INVESTIGATION OF THE EFFECT OF BLAST FURNACE SLAG, GLASS POWDER AND METAKAOLIN ADDITIONS ON THE ALKALINE ACTIVATION OF KAOLINITE

Zaid Mohammed Ali Kareem KAREEM

Karabuk University

Institute of Graduate Programs

Department of Metallurgy and Materials Engineering

Thesis Advisor:

Dr. Süleyman YAŞIN

May 2021, 86 pages

Kaolin based (hydrosodalite based) geopolymers are promising to produce greener building materials. In this thesis, kaolin based geopolymers with different amount of GGBFS, metakaolin and glass powder additions up to 40wt.% was produced and investigated to overcome the problems related to low reactivity of kaolin such as low strength. The samples produced by alkaline activation with NaOH solution and heat curing at 150 °C for 2h. Compressive strength, water-resistant, water absorption, FTIR, XRD, DTA-TG and SEM analyses were performed on the samples.

The sample with 30wt.% metakaolin exhibited a highest compressive strength (14 MPa). GGBFS addition were also enhanced the compressive strength. Sample with 20wt.% GGBFS showed 11.2 MPa, whereas the reference sample showed 3.1 MPa.

Glass powder additives didn't lead to a significant enhancement in the compressive strength. The water-resistant test showed good result for all samples, but the best values obtained with GGBFS addition. The results of the analytic tests such as XRD and FTIR proved the formation of the hydrosodalite phase as well as the presence of un-reacted kaolinite. DTA-TG analysis revealed that the thermal behavior of the samples was affected by the additives. SEM investigation showed the formation of hydrosodalite, remained kaolinite and microcracks. Results showed that the metakaolin and GGBFS are useful promoter for kaolin (hydrosodalite) based geopolymers produced by heat curing.

Key Words : Kaolinite, Geopolymer, Alkaline Activation, Hydrosodalite

Science Code : 9151

ÖZET

Yüksek Lisans Tezi

KAOLİNİN ALKALİ AKTİVASYONUNA YÜKSEK FIRIN CÜRUFU, CAM TOZU VE METAKAOLİN KATKISININ ETKİSİNİN ARAŞTIRILMASI

Zaid Mohammed Ali Kareem KAREEM

Karabük Üniversitesi

Lisansüstü Eğitim Enstitüsü

Metalurji ve Malzeme Mühendisliği Anabilim Dalı

Tez Danışmanı:

Dr.Öğr.Üyesi. Süleyman YAŞIN

Mayıs 2021, 86 sayfa

Kaolin bazlı (hidrosodalit bazlı) jeopolimerler, daha çevreci yapı malzemelerinin üretilebilmesi için umut vericidir. Bu tezde düşük mukavemet gibi kaolinin düşük reaktivitesiyle ilgili sorunların üstesinden gelmek için ağırlıkça % 40'a varan farklı miktarlarda GGBFS, metakaolin ve cam tozu ilaveleri içeren kaolin bazlı jeopolimerler üretilmiş ve incelenmiştir. Numuneler NaOH solüsyonu ile alkali aktivasyon ve 2 saat 150 ° C sıcaklıkta kür işlemi ile üretilmiştir. Numuneler üzerinde basma dayanımı, suya dayanıklılık, su emme, FTIR, XRD, DTA-TG ve SEM analizleri yapılmıştır.

Ağırlıkça %30 metakaolin içeren numune en yüksek basma dayanımı (14 MPa) sergilemiştir. GGBFS ilavesi de basma dayanımını artırmıştır. Referans numune 3,1 MPa basma dayanımı gösterirken ağırlıkça % 20 GGBFS içeren numune 11,2 MPa

basma dayanımı göstermiştir. Cam tozu ilavesi numunelerin basma dayanımında önemli bir artışa neden olmamıştır. Suya dayanıklılık testi tüm numuneler için iyi sonuç göstermiştir, ancak en iyi değerler GGBFS ilavesi ile sağlanmıştır. XRD ve FTIR gibi analitik testlerin sonuçları, hidrosodalit fazının oluşumunu ve reaksiyona girmeden kalan kaolinitin varlığını kanıtlamıştır. DTA-TG analizleri numunelerin ısı davranışının katkılardan etkilendiğini ortaya çıkartmıştır. SEM incelemeleri hidrosodalit oluşumunu, reaksiyona girmeden kalan kaolinitleri ve mikro çatlakları göstermiştir. Sonuçlar GGBFS ve metakaolinin yüksek performanslı kaolin(hidrosodalit) bazlı jeopolimerler elde etmek için kullanışlı bir geliştirici katkı olduklarını göstermiştir

Anahtar Kelimeler : Kaolinit, Jeopolimer, Alkali Aktivasyon, Hidrosodalit

Bilim Kodu : 91514

ACKNOWLEDGEMENT

I extend my sincere thanks and appreciation to Dr. Suleyman YAŞIN for his scientific and moral support. I wish him success from the bottom of my heart. Many thanks are also extended to all faculty members at the Institute of Graduate program and the Department of Metallurgy and Materials Engineering.

We acknowledge the Karabuk University, Turkey. This work was supported by “Karabuk University Scientific Research Projects Coordination Unit” under the project number (FYL-2020-2292).

I also extend my sincere thanks and gratitude to everyone who supported me during the master’s degree, especially my mother, father and my family. In the end, I would like to thank the generous Turkish people for their embrace and hospitality during my stay in Turkey.

CONTENT

	<u>Page</u>
APPROVAL.....	ii
ABSTRACT.....	iiv
ÖZET.....	vi
ACKNOWLEDGEMENT	viii
CONTENT	iix
LIST OF FIGURES	xii
LIST OF TABLES	xiv
SYMBOLS ANF ABBREVIATIONS	xv
PART 1	1
INTRODUCTION	1
PART 2	6
ALKALI ACTIVATION	6
2.1. A HISTORICAL OVERVIEW	6
2.2. PREPARATION AND REACTION MECHANISM OF ALKALI ACTIVATED BINDER	9
2.3. CHEMISTRY AND STRUCTURE OF ALKALI-ACTIVATED BINDERS	10
2.3.1. Low-Calcium Content	11
2.3.2. High-Calcium Content.....	11
2.4. ALKALI ACTIVATORS.....	12
2.4.1. Effect of Hydroxide Ions (OH ⁻).....	13
2.4.2. Effect of Soluble Silicates	13
2.4.3. Carbonates	13
2.4.4. Sodium Sulphate.....	14
2.5. APPLICATIONS OF ALKALI-ACTIVATED BINDER	14

	<u>Page</u>
PART 3	15
ALKALINEACTIVATION OF UN-CALCINED PRECURSORS.....	15
3.1. ALKALINE ACTIVATION OF FLY ASH	15
3.2. ALKALINE ACTIVATION OF SLAG.....	19
3.3. ALKALI ACTIVATION OF GLASS POWDER.....	23
4.4. ALKALI ACTIVATION OF KAOLINITE.....	25
PART 4	32
EXPERIMENTAL STUDIES.....	32
4.1. MATERIALS	32
4.2. SAMPLE PREPARATION.....	35
4.3. CHARACTERIZATIONS	38
4.3.1. Determination of Compressive Strength	38
4.3.2. Determination of Water Absorption and Weight Loss in Water	38
4.3.3. DTA-TG Analysis	38
4.3.4. XRD Analysis.....	39
4.3.5. SEM Analysis	39
4.3.6. FTIR Analysis.....	39
PART 5	40
RESULTS AND DISCUSSION	40
5.1. APPEARANCE OF THE SAMPLES	40
5.2. COMPRESSIVE STRENGTH RESULTS	41
5.3. WATER RESISTANCE AND WATER ABSORPTION OF THE SAMPLES	
.....	44
5.3.1. GGBFS Added Samples	44
5.3.2. Metakaolin Added Samples.....	46
5.3.3. Waste Glass Powder Added Samples	48
5.4. XRD RESULTS	49
5.5. FTIR RESULTS	51
5.6. DTA –TG RESULTS	53
5.7. SEM RESULTS	58

	<u>Page</u>
PART 6	67
CONCLUSION AND SUGGESTION	67
REFERENCE.....	69
RESUME	86

LIST OF FIGURES

	<u>Page</u>
Figure 4.1. XRD pattern of the kaolin.	33
Figure 4.2. XRD pattern of GGBFS.	33
Figure 4.3. XRD pattern of the waste glass.	34
Figure 4.4. XRD pattern of metakaolin	35
Figure 4.5. Steel mold.....	37
Figure 4.6. Sample before curing.	37
Figure 4.7. Experimental plan.	37
Figure 5.1. Appearance of the samples produced with different additives ; M; Metakaolin, G; Waste Glass powder and GGBFS; Ground granulated Blast furnace slag.	41
Figure 5.2. Compressive strength of the samples	44
Figure 5.3. Weight loss (wt.%) of GGBFS added samples	45
Figure 5.4. Water absorption (wt.%) of GGBFS added samples.....	46
Figure 5.5. Weight loss (wt.%) of metakaolin added samples.	47
Figure 5.6. Water absorption (wt.%) of metakaolin added samples.....	47
Figure 5.7. Weight loss (wt.%) of waste glass added samples	48
Figure 5.8. Water absorption (wt.%) of waste glass added samples	49
Figure 5.9. XRD pattern of the samples, K; kaolinite, HS; Hydrosodalite	50
Figure 5.10. FTIR spectrum of the samples.....	53
Figure 5.11. DTA curves of precursors, reference and waste glass powder added samples.	55
Figure 5.12. DTA curves of precursors, reference and metakaolin powder added samples	55
Figure 5.13. DTA curves of precursors, reference and GGBFS powder added samples	56
Figure 5.14. Thermogravimetry curves of precursors, reference and waste glass powder added samples.	56

	<u>Page</u>
Figure 5.15. Thermogravimetry curves of precursors, reference and GGBFS powder added samples.	57
Figure 5.16. Thermogravimetry curves of precursors, reference and metakaolin powder added samples	57
Figure 5.17. Microstructure reference sample. K; kaolinite , HS ; Hydrosodalite	59
Figure 5.18. Microstructure of 20wt.%GGBFS added samples	59
Figure 5.19. Microstructure of reference sample a) and 10wt.%GGBFS added samples b).....	60
Figure 5.20. Microstructure of 30wt.%GGBFS added samples. K; kaolinite, HS; Hydrosodalite	60
Figure 5.21. Microstructure of 40wt.%GGBFS added samples. K; kaolinite, HS; Hydrosodalite	61
Figure 5.22. Microstructure of 40wt.% Metakaolin added samples.	62
Figure 5.23. Microstructure of 30wt.%Metakaolin added samples. K ; kaolinite, HS ; Hydrosodalite	62
Figure 5.24. Microstructure of 40wt.% waste glass a), 40% Metakaolin b) and 40%GGBFS c) added samples (continue).....	64
Figure 5.25. Microstructure of 10wt.% waste glass added samples. K; kaolinite, HS ; Hydrosodalite	64
Figure 5.26. Microstructure of 30wt.% waste glass added samples. K ; kaolinite, HS ; Hydrosodalite	65
Figure 5.27. Microstructure of 20wt.% waste glass added samples.	65
Figure 5.28. Microstructure of 40wt.% waste glass added samples.	66

LIST OF TABLES

	<u>Page</u>
Table 4.1. Chemical composition of the kaolin	32
Table 4.2. Chemical composition of the GGBFS.	33
Table 4.3. Chemical composition of the waste glass powder.	34
Table 4.4. Chemical composition of metakaolin.	35
Table 4.5. Sample's series.....	36

SYMBOLES ANF ABBREVIATIONS

SYMBOLS

Al	: aluminum
C°	: centigrade degree
Si	: silicon
Mg	: magnesium
Ca	: calcium
O	: oxygen
OH	: hydroxide

ABBREVIATIONS

OPC	: Ordinary Portland Cement
NASH	: Sodium Alumina Silicate Hydrated
CSH	: Calcium Silicate Hydrated
CASH	: Calcium Alumina Silicate Hydrated
LTGS	: Low Temperature Geopolymeric Setting
AAB	: Alkali Activated Binder
AAF	: Alkali Activated Fly Ash
IR	: Infrared
XRD	: X-Ray Diffraction
FTIR	: Fourier-Transform Infrared Spectroscopy
DTA-TG	: Thermogravimetric & Differential Thermal Analysis
SEM	: Scanning Electron Microscope
BOF	: Basic Oxygen Furnace
EAF	: Electric Arc Furnace

PART 1

INTRODUCTION

The term “Geopolymer” was first assigned to synthetic inorganic aluminosilicate polymers that come from the chemical reaction known as Geopolymerization [1]. This type of polymeric material has a potential use in a number of applications, particularly as an alternative for ordinary cement and green building materials such as bricks [2,3]. In general, geopolymers are made up of a network of silicates composed of SiO_4 and AlO_4 tetrahedral, linked alternately with oxygen atoms [4]. The positive charged ions, such as Na^+ , K^+ , or Ca^{2+} , are essential to balance the negative charge of Al^{3+} , and they are located in the cavities of the structure [5]. There are numerous variables that affect the geopolymer manufacturing process such as type and composition of the starting materials, nature and concentration of the alkaline activator, temperature and curing time, etc. [2]. Although alkali activation was discovered earlier, the first time that the terms “geopolymers” or “geopolymerization” used was in 1979 by Davidovits [6]. Alkali activated materials had already been discovered by the Soviet Union in 1950 with the name of “Soil Cements” by the scientists Glukhovsky and Krivenko [6,7]. Those scientists are considered the first, who were wondering why the structures and buildings of antiquity, especially pyramids, lasted so long. This question stimulates their curiosity and accordingly, they were analyzed ancient buildings and found that their performance is, perhaps, due to the presence of free alkalis in ceramic matrices, and that might be the answer [6,7].

Generally, geopolymers have cementitious properties in relation to ordinary Portland cement (OPC). Also, as a distinctive feature, the emission of CO_2 is low during their production and this makes them as promising alternatives for ordinary Portland cement [8]. Comparing to the conventional cement, geopolymer production emission is less by about 80% [9].

Additionally, the studies have shown that such material have a considerable durability [10] and a list of others good properties such as good fire resistance [11], good resistance to freeze-thaw cycles, sulphate and corrosion resistance, low shrinkage [12] and easy adhesion to concrete, steel, glass and ceramics [13]. This technology has a great potential of produce environmentally friendly disposal waste material with high compressive strength and excellent durability [14].

It is useful to note here that geopolymers not only have good engineering properties, but their production costs are relatively low as well [15]. Rangan et al. have verified that there are economic improvements provided using geopolymeric concretes from fly ash [15]. They found such economic improvements are between 10% and 20% with respect to ordinary Portland cement [15].

Alkali activated binders are formed as a result of a series of reactions between the aluminosilicate rich raw material and the alkali activator. These reactions made Si-O-Al-O bonds that form alumina and silicate monomers [16]. The monomers then, by a polymerization process are turned into oligomers and then silicate polymers [17]. The reaction between aluminosilicate and alkali (Na_2O) usually forms alumina silicate hydrated (NASH) gel. This gel contains SiO_4 and AlO_4 tetrahedral units that are connected by sharing oxygen atoms. The negative charge of the matrix is balanced by adding cation such as Na^+ , K^+ and Ca^{2+} [18]. The binders that contain calcium ions, typically, have more complex reaction mechanisms. These systems produce CSH and CASH gels different than the usual amorphous NASH gel [19].

Geopolymers are obtained by alkaline activation of aluminosilicate raw material in a mild temperature within a specific formulation [20]. Although the setting and hardening mechanism of materials it's thought to depend on the type of raw material and activator. Different mechanisms have been proposed to understand the formation process of geopolymers. According to Davidovits [5], the geopolymer synthesis occurs in three steps [7,21];

- **Dissolution:** In this step, the dissolution of Si and Al atoms from the raw material happens under the influence of hydroxide ions and, thus ions are created.

- Transportation or orientation: Here, Concentration of raw material ions is converted into monomers.
- Polycondensation: this is a type of polymerization of monomers based on the functional groups of the reacted monomers and in which a polymeric structure is obtained.

In 1991, Davidovits stated that there are three different amorphous-semi-crystalline three-dimensional aluminosilicate structures geopolymer [18]. These are: poly (sialate), poly (sialate-siloxo) and poly (sialate-disiloxo).

Different reaction mechanisms have been proposed according to the ratio of silica and alumina in the raw material. When the ratio of silica and alumina is 1:1, the reaction with alkali forms ortho-sialate. This product also reacts with alkali to form a poly-sialate structure. However, when the content of silica and alumina in the raw material is in the ratio of 2:1, the reaction with alkali forms ortho-sialate-siloxo. It also reacts with alkali to form the poly-sialate-siloxo structure. When the content of silica and alumina in the raw material is in the ratio of 3:1, ortho-sialate and di-siloxonate are initially formed due to the alkali effect on the aluminum silicate material. These then undergo polycondensation and form poly-sialate di-siloxo. If silica: alumina ratio exceeds three, sialate link and poly (sialate-multi siloxo) are formed [22].

Kaolin is a mineral which conventionally utilized in industrial application such as production of porcelain [23]. Kaolin is soft, sedimentary rock [24]. Kaolinite occurred by rock weathering [24]. It is occurred generally by disintegration of K-feldspars, granite, and aluminum silicates [24]. Kaolin stands out for its early utilize, they constitute a majority clay in the first ten meters of the earth's crust [23]. Kaolinite is the main precursor employed in geopolymerization process [25]. Kaolinites frequently used in geopolymer formations but with its highly reactive phase as in calcined form [26].

The reaction of kaolinite minerals in alkali activation or geopolymerization is deeply related to the composition, as well as to particle size, surface area, porosity and crystal morphology [27]. Kaolin has low reactivity [28]. However, a sufficient thermal,

mechanical, or chemical treatment can be used to raise reactivity of clay particles [28]. Heating kaolin above 550 °C converts it into metakaolin due to the loss of structural OH⁻ groups. This process tends to be the most successful approach among past studies [28]. However, mechanical treatment can cause imperfection in kaolinite structure [28]. These changes can modify the porosity, morphology and surface area [29].

In general, calcinations process enhances the reactivity of the aluminosilicate precursor in geopolymerization reaction, and consequently, improving characteristics of geopolymer products especially compressive strength at early curing stages [30]. Calcination's process is responsible for the changes in the composition and structure of the material and cause a transformation from a crystalline structure to an amorphous more reactive structure [31]. However, the calcinations process of kaolin emits a large amount of CO₂ due to the need for achieving high temperatures and prolongs the duration of the manufacturing process as well as [32]. According to Davidovits et al. the calcinations process of metakaolin are function of time, temperature, and furnace technology [33].

All these constraints accompanied with calcinations process pushes researchers to find out new methods to avoid calcinations process and using starting materials sorted as natural precursor and without applying any pretreatment [34-36]. Geopolymers produced with un-calcined kaolin called as kaolin based geopolymers or hydrosodalite based geopolymers refer to final crystal structure [37]. Due to the low reactivity and slow reaction kinetics of kaolin, kaolin based geopolymers suffer lower strength by similar low-cost curing techniques generally applied for metakaolin based geopolymers [37].

In this study, it is aimed that the preparation of kaolin based (hydrosodalite based) geopolymer product with higher productivity (by rapid production) and higher performance than reported before. For this purpose, rarely used heat cure technique was used for sample to ensure rapid production. Samples cured at 150°C for two hours without pre or after drying process. In addition, kaolin blends with the more reactive solid precursors in various ratios for obtaining higher performance at final products. Influences of metakaolin, GGBFS (ground granulated blast furnace slag) and waste

glass powder additions on the mechanical properties and structure of the samples was investigated systematically. This study investigated the effects of the rapid heat curing technique and blending of different geopolymeric raw materials in kaolin based (hydrosodalite based) geopolymer synthesis together.

PART 2

ALKALI ACTIVATION

Alkaline activation can be defined as a chemical process in which aluminosilicate is mixed with an alkaline activator to produce a pasty product [38]. The properties of the resulting product (i.e., strength, fire resistance shrinkage and acid resistance) rely, mainly, on the activation process variables and, of course, the nature of aluminosilicate used [19]. This chapter introduces a theoretical background about alkali-activated materials. The first part of the chapter gives a brief review about the historical background of alkali-activated binders. This is followed by describing the reaction mechanism and the chemical structure of alkali-activated binders. The types of alkali-activators and the effect of each group are also described. At the end of the chapter, some essential applications of alkali-activators binders are given.

2.1. A HISTORICAL OVERVIEW

Alkali activated binders were first emerged in Europe, particularly in the western countries. In 1908, for the first time, Kühl [39] (who is a German chemist and an engineer) carried out studies on new generation of binders based on the reaction of materials containing alumina and silica with an alkali solution source. The binder prepared by Kühl can be considered as the first alternative to the ordinary portland cement (OPC) binders. The binder was producing by mixing blast furnace slag with alkali sulphate and carbonate and was finding that it has an effect similar to that of OPC binders [39].

Different from Kühl work, Purdon [40] in 1940s performed the most comprehensive study about this type of binders. The author activated thirty different blast furnace slag with a mixture of calcium hydroxide and different sodium salts and sodium hydroxide solutions.

Purdon found that the new binders give a similar development of compressive strength to that of OPC and have many advantages over Portland cementitious structures in terms of the emission heat, flexural strength and solubility [7,40,41]. However, in the 1959s, Glukhovsky [42] was the first who had explored the binders used in Egyptian constructions and ancient Roman. He concluded that the binders consist of aluminosilicate, similar to those of OPC. In addition, he concluded that the binders have crystalline regions of analcite (a type of rock that may interpret the durability of those binders). Depending on this investigation, Glukhovsky [42] developed a new type of binders (known as “soil–cement”). The word soil refers to the binder appearance which is like a ground rock and the word cement is used because of its cementitious capacity. This new binder was prepared using aluminosilicate from ground mixed with industrial wastes that are rich in alkalis [7].

Similar to Glukhovsky’s work, Malinowsky [43] had examined ancient structures repaired with ordinary cement. He observed that the repairing material was decomposed only after ten years, proving the low durability of OPC binders. It is helpful to emphasis here that many other authors have noticed the existence of analcime zeolites (about 40%) in the chemical composition of mortars used in Tel-Ramad (located in Syria) and ancient Jericho (the Jordan river valley) [7,44-46].

In 1981, Davidovits [47,48] proved that the acceleration of alkali activation development occurs after kaolinite-limestone-dolomite mixture calcinations and the product is alkali-activated binder. In 1983, Langton et al. characterized different historical building materials and found traces of alkali activation in some ancient building materials [49]. This has interpreted the high durability behaviors of ancient structural building materials [49]. In 1985, US army published a report dealt with importance and uses of binder’s materials produced by alkali activation technology. Such materials used as repair materials for runways defects [50]. In that same year, Davidovits and Sawyer [51] produced poly-sialatesiloxo materials with a high strength at early stages of curing. These materials are prepared by mixing GGBFS with abundance of Al^{+3} cation with strong alkali solution (such as NaOH and KOH with water and a sodium and/or potassium polysilicate solution). In 1986, Krivenko studied the $R_2O-RO-SiO_2-H_2O$ bonds on alkali activation in his Ph.D. thesis [52,53].

In 1987, Davidovits [46] has an attempt to investigate the reasons behind the exceptional durability of some ancient structural and building materials, comparing to those used in modern structures. He found that some of ancient materials (concrete and cement) have geopolymeric structure. In 1988, Kaushal et al. investigate by characterizing adiabatic temperature rises, hydration temperature and hydration products of fly ash and slag mixtures [54]. In 1989, a good amount of research has been performing about alkali-activated materials; Deja and Malolepsy demonstrated the chemical resistance of alkali-activated concretes to chloride ions [55]. Roy and Langton studied the usability of historic concrete as a repository material in tuff inside cemented structures [56]. Majundar et al. studied a hydration of $C_{12}A_7$ slag activation mixture to produce high strength and fast setting cement [57]. Finally, Talling and Brandstetr studied alkali activated slag clinker-free concretes, taking into account their practical applications and development [58].

In 1990, Roy et al. tried to shorten the setting time of concrete by developing formulations applied in alkali activation-based cement [59]. In that same year, Wu et al. studied early activation slag and a mixture of slag and cements [60]. They noticed that the present of activated blast furnace slag improve the mixture considerably in relation to ordinary Portland cement. In 1992, Roy and Silsbee examined, also, the role of alkali-activated based by-product materials [61], while Palomo and Glasser studied the parameters and properties of alkali-activated based metakaolin [62]. In the latter study, a higher strength at high curing temperature was observed [62]. In 1994, Glukhovsky, investigated the role of binder materials used in ancient Roman and Egyptian structural and building materials [63]. The author found that there were some indications about the possibility of using binders prepared from clays of aluminosilicates with low or free-calcium [63]. In 1995, Wang and Scivener investigated the microstructures of hydration alkali activated slag and concretes [64]. In the year after, Shi worked on the pores, permeability, and strength of alkali activated slag binders [65]. In 1997, Fernández-Jiménez and Puertas investigated the kinetics of alkali-activated slag cements at different temperature [66]. In 1998, Katz explored the microstructure of alkali-activated fly ash in normal environment to improve fly ash reactivity [67]. In 1999, Palomo et at el. showed in a publication that alkali-activated fly ash would be one of the promising ingredients in the cement of the future [68].

In 2000, Gong and Yang studied the influence of phosphate on alkali-activated red mud and slag mixtures [69]. In 2002, Krivenko and Kovalchuk studied the formation of zeolites and hydroxysodalite phases from fly ash alkaline activated at high molar ratios, $\text{SiO}_2/\text{Al}_2\text{O}_3$ (4.5-5) [70]. To date, the research work on activated-alkali binders is ongoing and most of the studies focus on developing a new mixture of this binder and still there are many research questions need to be answered.

2.2. PREPARATION AND REACTION MECHANISM OF ALKALI ACTIVATED BINDER

Alkali activated binder (AAB) may be prepared via two approaches. First is a one-part mixture. In this case, AAB forms only due to the combination of powder and water. Second approach is called 'two-part mixture'. As a main difference of the one-part method, here a combination of powder and alkali activator solution forms AAB [71]. Currently, the two-part mixture method is widely used and is considered the main and the most effective method. Accordingly, the most factories, especially those for precast production line, depend, essentially, on this method. However, while two-parts method have many advantages, it is important here to mention that the one-part mixture method can be viewed as a promising approach if the problem related to slow strength development is solved [7, 72].

So far, an explicit reaction mechanism that shows the formation of alkali-activated binders is not fully understood. Glukhovsky et al. proposed that the mechanism of AAB consists of destruction and condensation reactions [73]. The destruction occurs to the prime materials and converts them to low stable structural units. These structures interact with coagulation structures, forming the condensation structures. Generally, the first steps start by breaking Si-O-Si and Al-O-Si bonds. The breaking process occurs when the pH of the alkaline solution increases. So, Si-O-Si and Al-O-Si groups are transferred in a colloid phase. After that, the products are accumulated and interact with each other to make a coagulated structure, leading to generating a condensed structure.

Other authors are also in agreement with the mechanism proposed by Glukhovsky et al. [73] which is based on dissolution of silica, followed by the changing of phases and polycondensation [74,75]. Unfortunately, those phases generate almost at the same time, make their analysis individually difficult [71]. Fernández investigated the activation process of metakaolin [76]. Interestingly, the author reported different reactions when the sodium hydroxide is used as an activator. In the first case, Fernández noticed that there is an induction period following the dissolution of silica (when the accumulation of the destroyed products begins) [76]. In the second case, there is fast polycondensation reaction directly following the fast dissolution of silica phase.

For Criado et al., fly ashes activation process is drastically different than that of OPC hydration [77]. The product consists of the tetrahedral silica and aluminum in long polymeric chains. During the reaction between alkali and the alumina-silicate material, a nucleation happens where aluminosilicate solute is dissolved. When the formed nuclei get bigger, they begin to crystallize. However, this crystallization process is very slow and it takes a long time to be completed [77].

Many other authors explored the metakaolin activation process and agreed that the initial phase formed during the polymerization is later changed to a more ordered phase (second phase). They observed, however, that increasing $\text{SiO}_2/\text{Al}_2\text{O}_3$ ratio affects adversely the initial rate of reaction [78,79].

2.3. CHEMISTRY AND STRUCTURE OF ALKALI-ACTIVATED BINDERS

The family of alkali-activated materials is extremely broad in structure and chemistry. Therefore, to simplify the discussion of these materials in terms of the structure and chemistry, they are classified here in two groups according to calcium content [80]. This appears to be reasonable since calcium content is the main factor that determines whether the binder has a network structure or linear structure in terms of silicate structures.

2.3.1. Low-Calcium Content

Binders in this group are materials that have low calcium content. A good example of this group is F-type fly ashes [81]. The activated components of low calcium binders are primarily aluminum and silicon oxides. In low calcium systems, usually $(\text{Na or K})_2\text{O}$, Al_2O_3 , SiO_2 , H_2O bonds are formed. In practice, both the high alkaline environment and high curing temperatures are needed to trigger the reactions in the activation process of low-calcium materials. Three-dimensional inorganic alkali polymer materials (i.e., network polymer) are formed in the activation of low-calcium materials.

According to Glukhovsky [73], there are three stages of reaction mechanism describing the alkali activation process of low-Ca materials. The first stage of this mechanism is fragmentation and coagulation. The second is coagulation and condensation, and the third stage is condensation and crystallization.

In this type of alkali-activation systems, zeolite types such as hydroxysodalite, zeolite P, Na-cabasite, zeolite Y and fojasite are formed as the secondary hydration product. Alkali-activated low calcium bearing materials are disordered [82]. As the curing time increases, hydration products rich in silica are formed and the mechanical properties are directly affected [77, 83,84].

2.3.2. High-Calcium Content

High-calcium binders are rich in calcium and silicon oxides ($\text{SiO}_2+\text{CaO}>70\%$). These types of materials can be activated with alkalis under moderately alkaline conditions [85,86]. In high-calcium content systems, $(\text{Na or K})_2\text{O}-\text{CaO}-\text{Al}_2\text{O}_3-\text{SiO}_2-\text{H}_2\text{O}$ bonds are formed. The reactions products are mainly calcium silicate hydrate gel (C-A-S-H). This gel structure is similar to the gels obtained from Portland cement hydration [87].

Glukhovsky [88] and Krivenko [89] have proposed a model that explains the alkali activation of calcium and silicon-rich materials (blast furnace slag and calcareous fly ashes). In the model, the alkaline cation (R^+) works only as a catalyst. This is because

the cation exchange capacity of Ca^{+2} ions is high at the beginning of hydration reactions. As the reaction continues, alkaline cations are within the structure of the hydration products [88,89].

Fernandez-Jimenez et al. reported that the anion structure in solution is effective on the initial reactions of activation and setting time [90]. C-S-H gel (or calcium silicate hydrated) is the main hydration product formed. In addition to the C-S-H gel, secondary hydration products such as portlandite and calcium sulfoaluminate are also formed [91]. Comparing to OPC, the main hydration product of the binders formed from blast furnace slag is a structure similar to the main hydration product (i.e., C-S-H gel) of OPC. However, Ca/Si ratio ranges from 0.9 to 1.2 of the C-S-H gels and this ratio is lower than that formed by Portland cement hydration. In addition, as a result of the activation, the aluminum existing is presence in the structure of the C-S-H gel and forms the C-A-S-H structure. On the other hand, the secondary hydration products formed from the alkali-activation process of blast furnace slag depending on the chemical composition of the binder used and the type and concentration of the alkali activator. Further, the curing process varies depending on the conditions and pH value [92-94].

2.4. ALKALI ACTIVATORS

Caustic alkalis or alkaline salts are common compounds that are used in production of alkali-activated materials [86]. Glukhovskiy et al, classify alkali activator according to their chemical compositions into six groups including hydroxides, carbonates, sulfates and silicates [73].

The most common available and economic activators are those with sodium compound (NaOH , Na_2CO_3 , $\text{Na}_2\text{O}\cdot n\text{SiO}_2$ and Na_2SO_4). Of course, potassium exhibits similar properties of sodium compound [86]. However, using of potassium compounds is limited due to their unavailability and highly cost.

Since each group has a role in the preparation of alkali-activated materials, it is helpful to discuss their role in detail as shown in the following subsequent sections.

2.4.1. Effect of Hydroxide Ions (OH⁻)

One of the most used chemicals as a source of hydroxide is caustic soda. Commercial caustic soda is produced by the electrolysis of brine or sea salt. Except liquid phase, caustic soda is available commercially in two solid shapes: flake and beads. The presence of water dilutes NaOH concentration. The dissolution of NaOH accompanied with heat emission especially at a low concentration. Caustic soda can be used as an accelerator in OPC hydration. However, it causes a decrease in strength after 7 and 14 days of hydration. The use of caustic soda is usually applied by dissolving the anhydrous solid form in water [86].

The hydroxide ions in the alkali activation mechanism serves as a catalyst agent during the hydrolysis of Si-O-Si and Si-O-Al bonds, along with many other components in the dissolution of Si⁴⁺ and Al³⁺ cations. Further, hydroxide ions help to provide the conditions for initial dissolution and condensation reactions by increasing the pH of the medium [86-88].

2.4.2. Effect of Soluble Silicates

Sodium silicate is one of the most commonly used activators in the alkali activation of slag, fly ash and metakaolin [95-97]. The soluble property of silica in the activator influences the workability (consistency) of the mixture, setting time and strength development [30,96-99]. Sodium silicate can be diluted with water or diluted with sodium hydroxide to control the modulus value. It is important to mention here that the solution begins to gel when the pH drops below 10 [88]. The acidity of the solution (pH), in general, depends on the SiO₂/Na₂O ratio of the structure.

2.4.3. Carbonates

The components containing carbonate usually have a lower environmental impact than hydroxide or silicates due to the production processes. In addition, as distinctive feature, compounds containing carbonate have a lower pH value. Accordingly, it is considered less dangerous in terms of occupational health and safety. However, on the

downside, the reaction rate of the activators containing carbonate is slower than that of the sodium hydroxide and sodium silicate activators [100]. That might interpret why a little amount of research has been focused on the carbonate-based activators [100].

2.4.4. Sodium Sulphate

Sodium sulphate (Na_2SO_4) and calcium sulphate hemihydrates ($\text{CaSO}_4 \cdot 1/2\text{H}_2\text{O}$) can be used as an activator in alkali activation. Since the saturated sodium sulphate has a moderate pH value (about 7) than other hydroxide or silicate containing activators, the reaction rate is quite slow. When used as a gypsum activator, high amounts of hydroxide ions are required to increase the activation rate [73, 88].

2.5. APPLICATIONS OF ALKALI-ACTIVATED BINDER

Alkali-activated binders have been used for numerous purposes in various building and construction applications. These applications of alkaline-activated binders included: structural concretes, production of block elements, concrete roads, pavements, telephone and electricity poles, concrete pipe, refractory concrete, oil well cement, stabilization and solidification of harmful and radioactive wastes [71].

PART 3

ALKALINEACTIVATION OF UN-CALCINED PRECURSORS

Alkali activated products obtained by using un-calcined precursors have lower cost and lower CO₂ emission than product including calcined ones. The mentioned properties make these materials more feasible for mass production such as building materials. These starting materials are numerous. However, some of them have high availability with high reactivity such as fly ash, slag, waste glass powder and kaolin. This chapter reviews critically the relevant literature about these precursors respectively.

3.1. ALKALINE ACTIVATION OF FLY ASH

Fly ash is a fine powder. It is the main by-product of combustion process of pulverized coal which typically occurs in thermal power stations, petrochemical industry and electric power plants [101]. Chemically, fly ash is a pozzolanic material. This means that it produces cementitious phases when reacts with water and calcium [101]. The products of reaction share the same characteristics of portland cement. This main feature makes fly ash as an excellent choice for a wide range of applications in construction materials. Additionally, fly ash is one of the main ingredients of mosaic tiles, brick and hollow blocks [101]. Further, it is used in concrete and grout preparation to improve strength and to minimize segregation and makes it easier to pump. Also, it is used in cement production and added to soils as a stabilizer material [101]. According to this wide usage of fly ash, it is considered one of the most salable by-product materials [101].

The composition of fly ash is not constant; it changes according to the composition of unfired coal used and the amounts of impurities inside it [102]. The method of incineration, also, has a role in determining the composition of fly ash. For example,

fly ash produced via the combustion process of sub-bituminous coal is usually rich in calcium and contains less amount of iron in relation to that produced from bituminous coal [102]. In terms of chemical composition, fly ash contains, mainly, SiO_2 , Al_2O_3 , Fe_2O_3 , and CaO [102]. According to ASTM C618, fly ash may be classified into two types: C and F Class, the difference between them were calcium content, C class fly ash contain approximately more than 10 percent of calcium oxide while F class fly ash contain the less [103] For that reason, it is commonly known as high calcium fly ash. Class F, on other hand, is obtained from combustion of bituminous and anthracite coals and, accordingly, is termed as "low calcium fly ash"[104]. Aluminosilicate is the main component of Class F with a little amount Calcium Oxide (approximately less than 10 percent). This variation in chemical composition of fly ash makes its color varying from tan to dark grey [104].

Fly ash contains crystalline and amorphous (glassy) phases [105]. The crystalline phases are, generally, mullite, quartz and magnetite [105]. In the polymerization process, these phases are inactive during the early stage of dissolution and reaction [105]. However, the amorphous phases are reacted very fast and dissolved in alkali solution. Thus, it can infer that the glassy phase fly ash gives a good opportunity to investigate reaction mechanism (dissolution and polymerization) [105].

It is helpful to mention here that there are other distinctive features of fly ash such as fineness and uniformity [101]. Both are very important and are a direct result of a parameter called 'the loss on ignition (LOI)' [101]. This parameter determines the amount of un-burnt carbon remaining in the ash [101]. Fineness of fly ash mostly relies on the conditions of coal processing, especially the crushing and grinding process [101]. Finer gradation, typically, leads to a more reactive ash, containing a less amount of un-burnt carbon [101].

Alkali hydroxide or silicate solutions are usually used to activate fly ash. The activation of low-calcium fly ash forms a gel binder with highly cross-linked structures (e.g., tetrahedral N-A-S(H)-type gel structures) (N-A-S-H abbreviation of sodium aluminate silicate hydrated). This structure is approximately similar to that noticed as intermediates throughout the synthesis process of zeolites [106].

In 1999, Fan et al. reported that the reason of low activity of fly ash is due to two factors. First is the glassy surface layer that covers fly ash particles that protect the inside constituent of fly ash particle. Second, fly ash's silica-alumina is a glassy chain with a composition of high Si, Al and low Ca that works as a firm material. Accordingly, this chain of Al-Si must be broken up to show the active core of fly ash particles [107]. Fan et al. in their study used water-glass for its trait of rapid hydrolysis when is added to the mixture of fly ash- $\text{Ca}(\text{OH})_2$. The hydrolysis process released NaOH which increased basicity of the mixture. After hydrolysis process acidity value (pH) reaches about 13.10 meanwhile before water-glass addition PH value was 12.63 for $\text{Ca}(\text{OH})_2$ saturated liquid. The change in pH value toward more basicity plays main role in silica-alumina chain corrosion. In normal cement paste, pH of solution is low, so the speed of disintegration is also low [107].

Different that Fan et al. [107], Palomo et al. investigated, in the same year, the alkali activation of class C fly ash using four different activator solutions. These are NaOH (12M), KOH (18M), NaOH and sodium silicate and KOH and potassium silicate. The ratio of $\text{SiO}_2/\text{Na}_2\text{O}$ in NaOH and sodium silicate solution is 1.23. The ratio of $\text{SiO}_2/\text{K}_2\text{O}$ in KOH and potassium silicate is 0.63. Fly ash is mixed with immediately prepared activator for 2 min then the mixture is poured into a mold. The liquid-solid ratio is between 0.25 and 0.3. Samples are heated in close and high humidity system for 2, 5 and 24 hours at temperature of 65°C and 85°C . They reported that the increasing temperature accelerates fly ash activation, while the liquid-solid ratio does not have an appreciable effect [108].

Palomo et al. also reported that mechanical strength is affected by temperature and type of activator used. The results showed that samples activated by (NaOH+sodium) silicate gives a higher compressive strength, namely 68.7 MPa when is cured at 85°C for 24 hr., but its decreases when was cured at 65°C for the same period. Furthermore, samples activated by the other types of activator solutions showed a drastically change in compressive strength obtained under similar conditions in relation to the first one used [108].

Puertas et al. in 2000, studied the effects of different parameters on strength behavior and hydration product. The parameters explored in the study were fly ash/slag ratio, activation concentration and curing temperature [109]. The results reported by Puertas et al. showed that the compressive strength increases when slag relative ratio increases. However, the authors did not find an essential effect that is related to the compressive strength through increasing curing temperature. It is necessary to mention here that the compressive strength obtained from 50% of both fly ash and slag activated by 10 M of NaOH and cured at 25°C exhibit a high compressive strength (nearly 50 MPa at 28 days aging). This value slightly increases by 5 MPa at 90 days aging [109].

Fernández et al. produced concrete using alkali activated fly ash instead of Portland cement, although they produce samples of portland cement concrete for comparison. Two types of alkaline activator were used: 8M of sodium hydroxide or a mixture of 85% (12.5M) NaOH and 15% of Na₂SiO₃. The samples prepared by mixing ingredients under certain weight ratios. The results derived from compressive strength test showed superiority to fly ash concrete over Portland concrete. Compressive strength growing begins at a high rate of development for the first 24 hours then exhibits normal increment with time. This high rate of strength development attributed to the rapid reaction between fly ash and activator solution. The result showed significant change in compressive strength development for sample activated by a mixture of NaOH and Na₂SiO₃. This is attributed to the role of sodium silicates. Fly ash concrete showed lower value for modulus of elasticity when is compared to concrete of Portland cement. The pull-out test showed advancement of fly ash concrete over Portland cement concrete [110].

Komljenović et al. evaluated the influence of many various alkaline activators as well as the nature of fly ash on the properties of alkali activated fly ash. Alkaline activators used were Ca(OH)₂, NaOH, NaOH+Na₂CO₃, KOH and Na₂SiO₃ at various concentrations. The important parameters studied in alkali activator were the nature and concentration of activator solution, whilst fineness was taken as a parameter for fly ash. The result of compressive strength showed that the samples activated by Na₂SiO₃ have higher compressive strength. This is attributed to the presence of Si⁺ which has a higher rate of reactivity, and hence a higher compressive strength

obtained. The results, also, showed that amorphous phases are formed in all activators type with small amounts of crystalline phases [111].

De Vargas et al. investigated the influence of $\text{Na}_2\text{O}/\text{SiO}_2$ (N/S) molar ratio, curing temperature and ageing time on mechanical properties and microstructure of alkali-activated fly ash, it is observed that there is an important role for both temperature and ageing time. Samples showed a higher compressive strength as curing temperature and ageing time increase. Also, it was observed that an increment in curing time helps in the formation of new geopolymeric phases and improve compressive strength by the way [112].

3.2. ALKALINE ACTIVATION OF SLAG

Ferrous and nonferrous metallurgy originated slag are co-products or by-products of metallurgical processes that involve melting of metals at high temperatures following by a cooling process until solidified (through different cooling paths and methods). Slag can be exploited in a wide range of applications [113]. Many kinds of slag (such as blast furnace slag) exhibit both pozzolanic and latent hydraulic activities which make them attractive material for this field [113]. The chemical composition of slag is varying [113]. These variations may affect the major constituents such as lime, silica, alumina, and magnesia. Also, they affect the minor constituents [113].

Slag is classified according to two criteria which are the type of metals melt and cooling approaches used. First criterion is based on the type of melted metal. Second criterion is depending on the cooling approach [114].

Crystalline slag or air-cooled slag is a crystalline phase of slag obtained as a side-product of casting a molten metal into the trench. During the solidification process, water is sprayed over the surface of the slag to accelerate the solidification and causing deep cracks that ease crushing processes. The surface of this type of slag contains a cellular or vesicular structure formed by gas bubbles evaporation [114].

Granulated slag is glassy phase of slag and is obtained by rapidly quenching of molten metal in water or air. This type may contain a very small amount of crystalline phase. After the granulated slag is formed, water inside slag should be removed, then is dried and grounded before it is used as a cementitious material. After grinding, residual metallic particles should be removed by applying a magnetic field [114].

Expanded or foamed slag is obtained by controlling the quantities of water, air, or foam which is applied as a coolant in cooling process. The variations in the amount of coolant and the cooling rate cause changes in the properties of the formed slag. This product is more cellular and vesicular in structure than air-cooled slag, consequently it is lighter in weight [114].

Pelletized blast furnace slag is formed by a cooling method that involves using a limited amount of water to cool the molten mass slag. Then, the slag droplets are thrown through the air using a drum with fines rotating at high speed and hence pellets rather than solid mass are produced. The produced crystalline pellets can be controlled by a cooling process, and these pellets are preferred to use as aggregate. In the same manner, more vitrified pellets can be produced and these are more favored in cementitious applications, in term of chemical composition.

Yildirim et al. studied the chemical composition of steel slag and reported that both basic oxygen (BOF) and electric arc furnace slag (EAF). The major constituent for both BOF and EAF are calcium and iron oxides. Also, they reported that the ladle slag, which is prepared during the steel refining processes, has different chemical composition from BOF and EAF. The difference is initiated from the addition of different alloys to the ladle furnace in order to obtain different grades of steel [115]. Further, Yildirim et al. mentioned that the iron oxides content of BOF may be higher than 38%, relying on the furnace performance. The variation in oxides content is related to the specific amount of iron oxides in molten conditions which cannot be transformed to steel and remain in iron oxide phases. The BOF slag contains silica (SiO_2) from 7 to 18% (by mass) and 0.5 and 4% from Al_2O_3 and MgO , respectively. The highest content of free lime is about 12%. High of amount of lime or dolomitic lime are used in the operation of iron transformation to steel and, consequently, the

BOF slag content of BOF slag increases to be more than 35% [21]. Further, the same authors reported that the chemical composition of EAF slag is relying on the chemical composition of recycled steel because the electric arc furnace steel-making process used a steel scrap recycling to produce steel of different grades. They summarized the typical content of chemical constituents of EAF slag as follow: FeO ranges between 10-40%, CaO between 22-60%, SiO₂ between 6-34%, Al₂O₃ between 3-14%, and MgO between 3-13%. EAF slag contains also different oxides as impurity such as MgO, SO₃ and MnO which existed in small amounts [115].

The alkali activated slag cements show several technical features in relation to OPC (ordinary Portland cement). The characterized alkaline activation of Slag (AAS) has a fast and high mechanical strength development, low heat of hydration, good chemical resistance, high bond strength at aggregate/matrix interface, and finally, a good resistance to freeze/thaw cycles [116].

Collins et al. reported that the slag activated by powder sodium silicate and lime slurry showed a better workability with time in comparison to other mixtures. At 30 min, the sample activated by powder sodium silicate and lime slurry shows a better slump than the previous time. This is a reasonable development in terms of workability because it refers to further dissolution and reaction between powdered sodium silicate and the water, at 120 min, the sample slump is lowered but remains higher than other mixture. Further, in that same study, the compressive strength was investigated, the sample activated by powder sodium silicate and lime slurry gives the highest value of compressive strength, exceeding OPC and samples activated by other materials [117]. Further, Collins et al. investigated the compressive strength development as a function of different curing conditions. It was noticed that there is a difference in strength between samples cured by exposed curing method and those by sealed and bath methods. Both of them make a specific change on the sample activated by powder sodium silicate and lime slurry. However, the bath and sealed curing methods give the best strength development in relation to exposed method [117].

Fernández-Jimenez et al. investigated the influence of a series of factors that control the mechanical strength development of alkali-activated slag cement mortar. They

noticed that unfamiliar results related to the selected factors. For the specific surface factor, slag of 450 m²/kg surface area show average values of strength greater than those of slag with 900 m²/kg. Also, the results show that, for samples with 4% activator concentration, the values of mechanical strengths (flexural and compressive) are larger at curing temperature of 25°C. In terms of the type of activators used, the Na₂SiO₃.nH₂O+NaOH activator gives the highest strength values in all condition used in the experiments, while, Na₂CO₃solution and NaOH activator gives the lowest strength values [118]. Interestingly, the results reported in Fernández-Jimenez et al. proved that the mechanical strength increased with reaction time [118]. The study also shows that the nature of alkaline activator has a higher effect in relation to another factor. This factor statistically has more significant effect on mechanical strength development. Activator concentration comes after, showing a moderate effect and then curing temperature and specific surface has the lowest effect. Hence, the chemical nature of alkaline activator can be considered as the most effective factor [118].

Different than the previous studies, Aydın and Baradan studied the effect of two different methods of curing (autoclaves and steam) on the alkali-activated slag mortars [119]. Regarding the curing methods, the results of Aydın and Baradan showed a higher compressive and flexural strength for OPC mortar samples cured by steam than those cured by autoclave. The reason of this behavior is that the hydration chemistry is changed considerably as the temperature and pressure increase [119]. The formed structure (C-S-H) transformed to a crystalline structure (α -calcium silicate hydrate), resulting in a high percent of porosity and a dropping in strength. Aydın and Baradan studied the effectiveness of curing methods used on compressive and flexural strengths. The result showed that at low modulus of silica ratio (0 and 0.4), the autoclave curing method gives excellence values comparing to steam curing method. But, for high modulus of silica ratios, both methods gave approximately similar compressive and flexural strength [119].

Panagiotopoulou et al. investigated the influences of both Si/Al ratio and kind of alkaline activator used on dissolution of precursor ions and compressive strength development of slag based geopolymer. The result derived from leaching process showed that the slag has considerable dissolution ability in alkaline medium, especially

in NaOH. The results proved that the compressive strength is highly affected by the presence of Si in alkaline activator solution and, also, Si/Al ratio and type of alkaline ions. The optimum value of Si/Al ratio was 3.5 at this ratio compressive strength was 112 MPa. Samples activated by 100% NaOH have a higher compressive strength than these activated by 50%NaOH and 50%KOH [120].

Shi investigated alkali-activated slag mortars. Alkaline activator used was a mixture of NaOH, Na_2CO_3 and $\text{Na}_2\text{SiO}_3 \cdot 9\text{H}_2\text{O}$ [121]. Shi results showed that the optimum type of alkaline activator used was Na_2SiO_3 . Results of pore structure show that the pore structure depended on the type of alkaline activator used. Samples of sodium silicates solution give a lower and finer porosity, whereas NaOH gives a higher and coarser porosity [121].

3.3. ALKALI ACTIVATION OF GLASS POWDER

Glass is an amorphous solid generally obtained by melting silica with oxides, it is made by cooling a molten viscous material of a particular composition to below glass transition temperature, without leaving time to form regular crystal structure [122,123]. Due to its high content of silica, many researchers were interested in employing glass in alkali activation technique [124,125]. Below selective researches that dealing with glass as a main source of precursor or additive.

Chen explored the influence of curing temperature and duration over the performance of compressive strength for alkali activated glass inorganic binder. The result of compressive strength presents a primarily affect for curing temperature, duration and alkali content in activator. The result showed the optimal curing period to obtain best compressive strength was reduced whenever curing temperature increased. The optimum conditions recorded were 4% alkali content, 60°C of curing temperature and 72 hours of curing duration where the compressive strength obtained at 28 day was 124.65 MPa [126].

Si et al. tried to use waste glass powder as a replacement precursor material in metakaolin based geopolymer to improve sustainability of geopolymer. 4 amount ratio

of waste glass were replaced with metakaolin, these amounts were 0%, 5%, 10%, and 20% by the total mass of precursor used. The results showed that the addition of waste glass powder increases the workability of paste, this is due to the smooth surface and tiny size of glass particles, so that the water amount required for reaching desired workability would be reduced. Another important finding was observed related to the reduction in time required for initial and final setting; this finding was attributed to the low reactive aspect of waste glass. The higher compressive strength was recorded for samples of 5% of waste glass replacement, any further replacement doesn't showed improvement in compressive strength, on contrary the strength was tending to drop down at 10% and 20% of waste glass replacement, this was attributed to increasing amount of un-reacted glass and reducing interface contact between glass and gel phase [127].

Dipten et al. tried to produce geopolymeric concrete that are suitable for pre-casting production. Author used waste glass as a precursor and sodium hydroxide and water glass were used as alkaline activator. Concentration of alkali activator were 6M and 8M, the samples were prepared by curing at 65 °C and at ambient for 72 hours to study the difference between both curing temperature. Sand was used as a filler, its added in ratio to binder of 1:2.75 (binder: sand). Fly ash based geopolymeric concrete was prepared under similar condition for comparison. The compressive strength was conduct at 3rd, 7th and 28th days. The results showed the samples of high curing temperature gaining early strength development that was suitable for pre-cast production. Also, the result presents the molarities effect of 8M was better than 6M, so that the compressive strength obtained at 8M was 64.6MPa for samples of waste glass based geopolymer [128].

Bilondi et al. investigate the possibility of using a glass powder based geopolymer to enhance the mechanical properties of clay soils. The results showed all samples of recycled glass had improvement in comparison with reference samples. The optimum ratio of recycled glass was recorded at 15% and any excessive increment of recycled glass more than 15% was behaved as un-reacted material or filled [129].

Si et al. investigate replacement effect of 0, 5, 10 and 20 % of glass powder in metakaolin based geopolymer. Activator solution used was a mixture of sodium silicate and sodium hydroxide. The result of mechanical properties showed small amount of glass powder below 10% present slightly increases in mechanical properties. Thus, the high content glass decreased the mechanical properties due to the raising quantity of un-reacted glass powder. The waste glass powder replacement showed a formation of denser gel in comparison with samples doesn't involve waste glass powder [130].

4.4. ALKALI ACTIVATION OF KAOLINITE

Kaolinite is a layered mineral of silicate clay formed by the natural chemical reaction of feldspar or other minerals of aluminum silicate [131]. Typically, it is white, with often a red impurity attributable to iron oxide, or blue or brown impurity owing to another mineral [131]. Kaolinite investigated in field of alkali activation technique [36] and geopolymer production [132]. The main determination of using un calcined kaolinite as a main precursor is its aspect of low reactivity. Many researchers worked on increasing the reactivity of kaolinite to be exploited in modern industrial application.

Heah et al. studied the effects of certain ratios of NaOH on kaolin-based geopolymer properties. It's observed that the samples durability affected by S/L, NaOH Molar and $\text{Na}_2\text{SiO}_3/\text{NaOH}$ ratio. The results of compressive strength behavior indicate that the compressive strength increase with the ageing time [133]. They caused that to the low reactivity of kaolin which leads to longer time consumed to complete geopolymerization reaction. Samples of 0.24 $\text{Na}_2\text{SiO}_3/\text{NaOH}$ ratio and 1.20 S/L ratios give the highest compressive strength but less workability, while samples of 0.24 $\text{Na}_2\text{SiO}_3/\text{NaOH}$ ratio and 0.60 S/L ratios give the lowest compressive strength and highly workability [133].

Slaty et al. attempted to produce low-cost construction materials kaolinite with a sodium hydroxide solution as a chemical activator. They studied the influence of the most affected parameters of synthesis and treatment on the progression of compressive

strength. Silica sand was used as a filler material and a NaOH is used for alkali solution preparation by diluted with distilled water [134]. Slaty et al. found that the compressive strength is improved and increases depending on NaOH contents. The greatest compressive strength gained was 33 MPa for the samples containing 16% mass ratio of NaOH. The result showed that, the more NaOH content, the compressive strength decreases. They found also that the addition of silica sand powder to the mixture can play an important role in improving compressive strength and workability. The result reveals that both curing temperature and time have impact on the compressive strength result [134].

Again, Slaty et al. studied the behavior of alkali activated cement produced from kaolinitic clay. In the study, the authors used two series of sample, one with silica sand as filler and the other without [135]. They prepared samples in similar ways mentioned previously in the work of the same authors (i.e., Slaty et al. [134]). The result showed that shrinkage behavior shows clearly evidence about the importance effect of sand filler to reduce shrinkage [135]. Another durability test was performed under two different environmental conditions. The first is at ambient conditions and the second one is at wet conditions. The results showed that, at ambient conditions, the samples with silica sand have a higher compressive strength values than the samples without silica sand. [135].

Heah et al. inspected the impact of curing process on kaolin-based geopolymer. A mixture of NaOH and Na_2SiO_3 was used as activator. The compressive strength results revealed that at room temperature, kaolinite exhibits very low dissolution, and the hardening becomes tangible after 7 days of ageing accompanied with slightly increase in compressive strength. The samples cured at 80°C for 3 days showed a decrease in the strength when they are ageing for 28 days. But, when the samples are cured for 2 days, there is no significant change observed in the compressive strength between 7 and 28 days. This information gives a clear explanation about unfeasibility of long curing. A similar result was observed for the samples cured at 100°C for 2 and 3 days [136].

Mat Daud et al. try to study the influence of mixing kaolin-based geopolymers with epoxy-layered silicate nano-composites on the mixture compressive strength. The results of the compressive strength showed that the samples of nano-composites without kaolin based geopolymeric filler give a lower compressive strength (up to 24.26Mpa) in comparison to samples with geopolymeric contents which give 36.65MPa. The strength modulus of samples with kaolin based geopolymeric filler showed an enhancement over the others [137].

Different than the reviewed studies, Heah et al. tried to improve the ability of kaolin to react with alkaline activator solution using mechanical activating process. The kaolin powders are treated mechanically to be activated by applying milling process for varied periods of time (from 1 to 5 hr.) [138]. The result of compressive strength indicated that the mechanical activation process stimulates the kaolin to react faster and the dissolution and solidification process to be achieved rapidly. The results showed that the longer the mechanically-activating time the better compressive strength obtained [138]. Hounsi et al. also investigated both mechanical activation and curing process. The compressive strength results showed superiority for milled samples over un-milled samples under all the studied conditions [139]. Heah et al. investigated the influenced of mechanically-activated kaolin over compressive strength and morphological properties [28]. The results showed a significant superiority of mechanically activated kaolin over non-mechanically activated, also earlier setting has reached and faster strength growing [28]. SEM image of kaolin raw materials showed the presence of needle-like and plate-like particle but after milling the result showed distortion in morphologic properties and some particles seems to be rounded [28]. The main result was most of particle showed decreasing in size [28]. This agreed with results obtained from compressive strength tests [28].

Boutterin and Davidovits developed a new technique called low temperature geopolymeric setting (L.T.G.S.). They mixed the soils that include kaolinite mineral with NaOH based activator and compressed batches inside a mold of desired shape, often the result was satisfied after curing. Particularly, mechanical strength obtained was enough to use as block of bricks [140]. They found that the properties influence

by amount of precursor in the mixture, amount of NaOH in mixture, resting time before curing, curing temperature and curing period [28].

Marsh et al. investigate the feasibility of new route to produce hydrosodalites suitable for extrusion process. The kaolinite used in this experiment was un-calcined and activated by using NaOH solution and taken into account the workability which should be enough for extrusion. The kaolin was subjected to drying at 105°C before mixing with alkaline solution for activation. Alkaline solution was added to each 25g of kaolin. The concentration of NaOH increases according to the increment in Na: Al to obtain a workability suitable for extrusion process. The mixture of kaolinite and alkali activation was blended for 3 min to get a consistent mix for extrusion, then was poured into a mold and cured at 80°C for 24 hours. However, the results obtained from XRD showed a formation of hydrosodalite. The study of Marsh et al. showed that there was an inverse relationship between consumed kaolinite and formation of hydrosodalite as and Na:Al ratio increases [35].

Marsh et al. investigated the alkali activation of kaolinite, montmorillonite and illite individually. The purpose of this experiments was to inspect and analyse the difference in phases formed from samples of mixing clay minerals and individual clay minerals. Clay minerals were activated using NaOH solution. The activated kaolin showed a formation of hydrosodalite as a major phase while the kaolinite was consumed gradually. The results are confirmed by SEM which shows the formation of 0.5-1 µm crystals. However, activated montmorillonite showed geopolymeric phases as a major and portion of montmorillonite were consumed and the remain stay un-reacted. XRD of Illite precursors showed illite as a major phase and quartz, microcline and kaolinite were as a minor, but activated illite does not show geopolymeric phases. The results obtained from XRD of activated mixture of kaolinite/montmorillonite/illite showed that the main phase produced was 8:2:2 hydrosodalite. All phases of clay minerals were not completely consumed [141].

Shaqour et al. investigate the alkali activation of kaolinitic clay using alkaline mixture of hydrated lime $\text{Ca}(\text{OH})_2$ and sodium carbonate Na_2CO_3 . The research involves using natural clay for comparison with kaolinitic clay. Certain amount of granite added as a

filler. The result obtained from XRD and SEM of showed that the alkali activation of natural clay produces hydroxysodalite and this proves the interaction between NaOH and kaolinite instead of CaCO_3 and there is not any impact for the formation of pirssonite. The samples activated using a mixture of $\text{Ca(OH)}_2/\text{Na}_2\text{CO}_3$ exhibits a compressive strength of 21 MPa and this value was 35% less than compressive strength obtained from samples activated by NaOH. Durability test was performed and the results showed a decrease in the strength of the samples soaked in water for 24 hours (from 34 to 22 MPa for those activated by NaOH, and from 21 to 11 MPa for samples activated by a mixture of $\text{Ca(OH)}_2/\text{Na}_2\text{CO}_3$) [142].

Esaifan et al. studied the development of un-treated kaolinite alkali activation by NaOH solution. They used kaolinitic clay as well as standard kaolinite as a reference for comparison also silica sand was used as a filler to evaluate the difference stability and strength [36]. XRD patterns results for both standard kaolinite and kaolinitic clay alkali activation showed a complete transformation of kaolinite into hydroxysodalite. The results proved that the standard kaolinitic clay of 98% kaolinite required 41% of NaOH ratio to achieve this complete transformation of kaolinite. However, only 28% of NaOH ratio is needed for natural kaolinitic clay (which contains 68% of kaolinite) to achieved complete transformation of kaolinite into hydroxysodalite [36]. Results obtained from compressive strength showed that the compressive strength increases with water ratio and a complete transformation of kaolinite into hydroxysodalite occur at 28% NaOH ratio. The optimum value of NaOH is 14% which giving a higher dry compressive strength (up to 48MPa) [36].

Ramasamy et al. studied the effect of kaolin (S) to the alkaline (L) ratio on the behavior of kaolin-based-geopolymer. Hardness and flexural strength were inspected under varied S/L ratio from 0.7 to 1.1. Geopolymer paste was coated over painted wood substrate and placed in the stream of hot air for 72 hours. Results of vickers hardness test showed a higher value for samples mixed at 0.7 ratio. This is attributed to the good workability that allows aluminosilicate to dissolve, forming hydrosodalite. The results indicate that when the ratio increases, the hardness recorded decreases and cracks starts appearing for samples mixed below 0.6 at under the specified curing condition. The

flexural strength results showed similar behavior and hence support previous analysis [143].

Jaya et al. investigated the role of sintering temperature on mechanical properties and of the geopolymeric ceramic produced. They used kaolin as a precursor and NaOH/Na₂SiO₃ as an activator. The geopolymeric sample were subjected to a milling and sieving before were compacted at 4.5 tons for 2 minutes. Finally, sintering process is carried out at temperature between 900-1200°C for 3 hours of soaking and cooling. The results proved that the samples sintered at high temperature give a lower density and vice versa. This inverse relationship is attributed to the closed pores creation at high sintering temperature and losses density while at low sintering temperature open pores were created, so the density is higher. The results showed that flexural strength increases with sintering temperature. At 900°C, flexural strength obtained is 37.11 MPa but at 1200°C the flexural strength obtained is 88.47 MPa [144].

Recently, in 2019, Tiffo et al. investigated the physical and mechanical properties of kaolin-based-geopolymer produced using amorphous aluminum hydroxide Al(OH)₃ and aluminum oxy hydroxide γ -AlO(OH). Kaolin and aluminum oxy hydroxide were milled together and sieved to 90 μ m. Alkaline activator synthesized by dissolving NaOH pellets with H₂O and Na₂SiO₃. The results obtained from compressive strength test showed that the samples cured at 60°C and without aluminum exhibit good compressive strength in comparison with sample contain aluminum and cured at same temperature. But, at high heating temperature more than 1100°C, compressive strength and volume stability of samples contained aluminum were enhanced [145].

In 2019, Shamala et al. explored the effect of NaOH morality on compressive strength and bonding force of kaolin-based geopolymer that coated over lumber wood. The flexural strength results showed that NaOH molarities plays a significant role in the mechanical strength behavior. The optimum concentration obtained for NaOH was 8M, the samples at this molarities recorded higher strength. The results derived from adhesive bonding test showed the best adhesive strength was at 8M. It was observed that the adhesive bonding force for samples activated by 8M NaOH molarities have grew with ageing time; this was not noticeable for other investigated samples [146].

Heah et al. investigated the effect of alkaline activator concentration on mechanical properties of kaolin based geopolymer. Alkaline activator used is composed of NaOH and Na₂SiO₃. NaOH solution was prepared in different concentrations varied from 4 to 16M [147]. Interestingly, the results derived from compressive strength agreed with those of Shamala et al. [146]. Both studies show that the compressive strength is affected significantly by alkali activator concentrations. The values obtained before 7 days ageing was too poor although a bit increments observed for samples of 6M and ageing more than 7 days. This is attributed to the initial reaction as well as the slowly dissolution of kaolin. Another observation was recorded at 8M that the values of compressive strength obtained showed uniformed and considered increases with ageing time due the abundance of OH⁻ which increases the dissolution of Al⁺³ and Si⁺⁴ from kaolinite structure. Higher compressive strength obtained at optimum value of 8M and 180 days ageing was 3.98 MPa [147].

Okoye et al. studied the feasibility of producing green concrete from fly ash/kaolin based geopolymer. Also, they investigated the influences of silica fumed presence in fly ash/kaolin based geopolymer in term of mechanical properties. Compressive strength results for flyash/kaolin based-geopolymer concrete samples showed higher values when fumed silica are used, the results proved there was a deep influence of compressive strength with time to superplasticizer amount uses and the higher compressive strength obtained when naphthalene super plasticizer was used. Finally, the compressive strength recorded decreases after at high amount of superplasticizer addition [148].

PART 4

EXPERIMENTAL STUDIES

4.1. MATERIALS

Kaolin was used as a main solid alumina silicate precursor and GGBFS, waste glass powder and metakaolin used as additives.

High purity fine kaolinite powders with 93% by volume below 2 μm particle sizes were used as a source of alumina and silicate. The chemical composition of kaolin present in table 4.1. The XRD pattern of the kaolin used is given in Figure 4.1. In the XRD pattern of kaolin, only peaks of the kaolinite mineral were detected.

Table 4.1. Chemical composition of the kaolin.

Chemical Composition (wt.%)									
Al₂O₃	SiO₂	P₂O₅	SO₃	K₂O	CaO	TiO	Fe₂O₃	Others	L.O.I
36.9	46.1	0.5	0.5	1.07	0.03	0.5	1.6	0.05	12.75

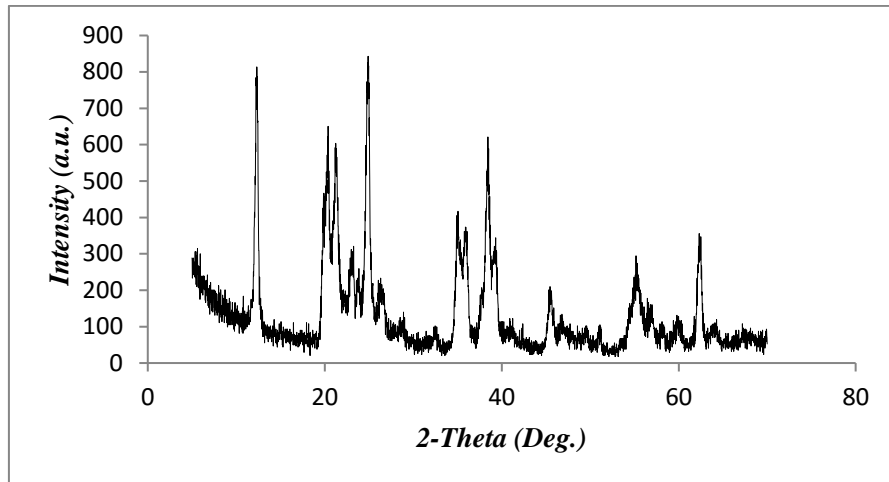


Figure 4.1. XRD pattern of the kaolin.

Origin of the GGBFS is Iron and Steel industry in Karabuk-TURKEY. $D_{(0.5)}$ value of the GGBFS is 13,5 μm . The chemical composition and XRD pattern of GGBFS is present in table 4.2 and Figure 4.2, respectively.

Table 4.2. Chemical composition of the GGBFS.

Chemical Composition (wt.%)										
MgO	Al ₂ O ₃	SiO ₂	SO ₃	K ₂ O	CaO	TiO	MnO	BaO	Fe ₂ O ₃	Others
4.9	11.1	37.1	1.6	1.4	38.9	0.4	2.3	1.05	0.7	0.1

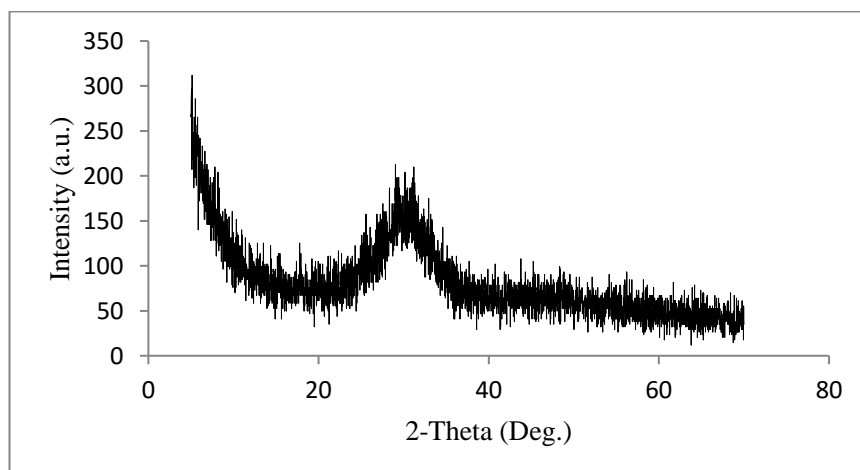


Figure 4.2. XRD pattern of GGBFS.

Waste glass powder used in these experiments is delivered from recycled window flat glass that obtained by ball milling waste flat soda-lime-silica glass to 30 to 70 μm . The chemical composition and XRD pattern of the waste glass is present in table 4.3 and Figure 4.3, respectively.

Table 4.3. Chemical composition of the waste glass powder.

Chemical Composition (wt.%)								
Na ₂ O	MgO	Al ₂ O ₃	SiO ₂	SO ₃	K ₂ O	CaO	Fe ₂ O ₃	Others
13.9	3.4	1.2	70.2	0.2	0.6	10.02	0.1	0.02

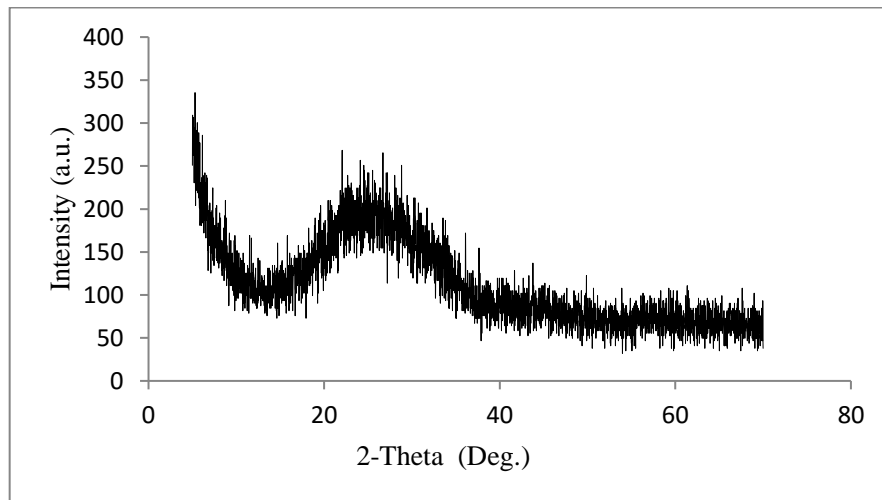


Figure 4.3. XRD pattern of the waste glass.

To produce metakaolin the kaolinite powders placed in the oven where heated to 750°C at a rate of 5°/min. and kept at this temperature for 6 hours. After 6 hours, the powders were naturally cooled to the room temperature in the oven. The chemical composition and XRD pattern of the produced metakaolin powders are given in Table 4.4 and Figure 4.4, respectively.

Table 4.4. Chemical composition of metakaolin.

Chemical Composition (wt.%)									
MgO	Al ₂ O ₃	SiO ₂	P ₂ O ₅	SO ₃	K ₂ O	CaO	TiO	Fe ₂ O ₃	Others
0.3	44.4	51.2	0.4	0.2	1.06	0.04	0.50	1.6	0.05

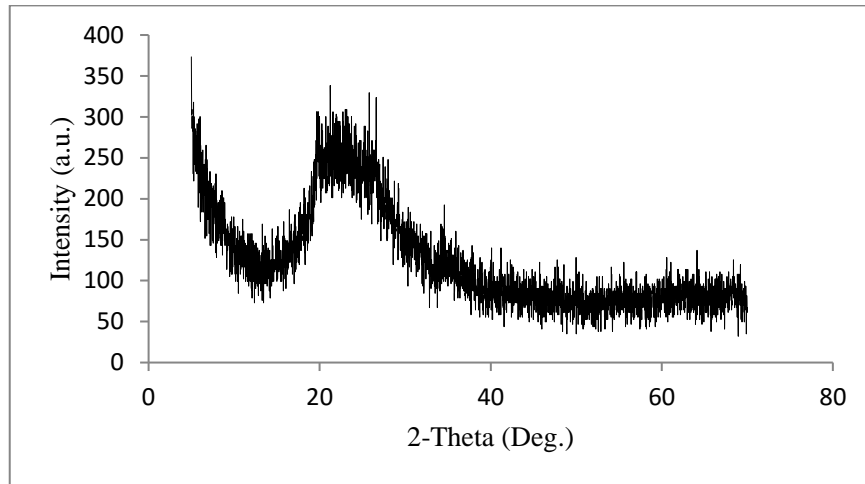


Figure 4.4. XRD pattern of metakaolin.

For preparing alkali activator solution sodium hydroxide pellet of Merck brand with 99wt.% purity and distilled water was used.

4.2. SAMPLE PREPARATION

Three types of samples according to its composition were produced, these were GGBFS, waste glass powder and metakaolin added samples. Each one of these samples branched into four sub-samples according to the amounts of additives added as well as reference samples which doesn't contain any additives with kaolinite (Table 4.5).

Table 4.5. Sample's series.

No.	Additive	Additive ratio (wt.%)
1	Reference (without additive)	0
2	GGBFS	10
3	GGBFS	20
4	GGBFS	30
5	GGBFS	40
6	Metakaolin	10
7	Metakaolin	20
8	Metakaolin	30
9	Metakaolin	40
10	Waste Glass Powder	10
11	Waste Glass Powder	20
12	Waste Glass Powder	30
13	Waste Glass Powder	40

The production procedure involves mixing pure kaolinite powder with additives in certain amount. Each additives material was mixed with kaolin in four different percentages by weight, namely: 10%, 20%, 30% and 40%. Solid precursor and additives mixed by electrical mixer for five minutes to obtain homogeneity. NaOH solution was prepared by dissolving sufficient amount of NaOH solid granules with distilled water in a closed bottle in order to avoid evaporation initiated from exothermic reaction. The amount of water in the samples was fixed 70wt.% by weight of kaolin to obtain sufficient workability suitable for plastic forming process. Sodium hydroxide was fixed at 24wt.% of the kaolin to obtain fixed molarities or fixed $\text{Na}_2\text{O}/\text{Al}_2\text{O}_3$ molar ratio at the samples to compare the role of additives.

Prepared solid mixtures and liquid phases were mixed together in a plastic container. The mixing step continues for 5 minutes then plastic consistency obtained which should be suitable for forming process, the plastic mixtures placed in steel molds (Figure 4.5) to obtain 10mm diameter and 20mm length cylindrically shaped samples (Figure 4.6). Formed wet samples directly dried in ventilated oven for 2 hours at 150°C without pre-drying process. After that, the samples removed from the oven and leaved to cool before conducting mechanical and analytical tests. (Production process of the samples is given in Figure 4.7).



Figure 4.5. Steel mold.



Figure 4.6. Sample before curing.

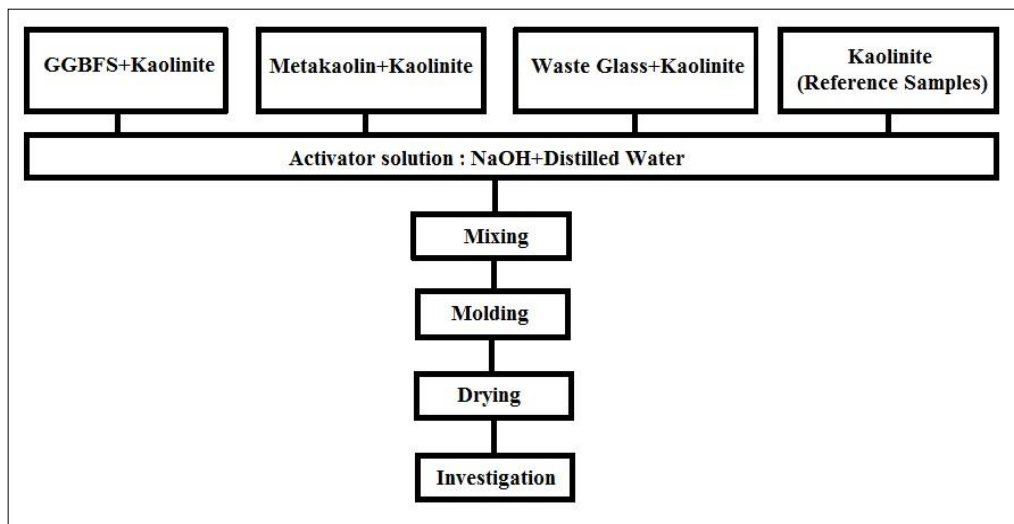


Figure 4.7. Experimental plan.

4.3. CHARACTERIZATIONS

Compressive strength, water absorption, weight loss in water, DTA-TG, XRD, SEM and FTIR analysis applied in this work.

4.3.1. Determination of Compressive Strength

The compressive strength test was carried out with a Zwick / Roell 600 kN capacity test device at a constant speed of 1.00 mm/min. The highest strength achieved until the samples were damaged was recorded. The experiments were carried out with three samples and the average values were taken.

4.3.2. Determination of Water Absorption and Weight Loss in Water

In this test, the samples weigh after drying process recorded values which are denoted by (W_i), then soaking samples in water (completely immersion) for 1 day then samples removed and weigh it again, the recorded weights denoted by (W_s). The percentage of water absorption is calculated by the equation below.

$$\% \text{ Water absorption} = ((W_s - W_i) / W_i) * 100 \quad (4.1)$$

To calculate weight loss percentage in water medium, dried wight measure and denoted by (W_i), then samples immersed in water for up to 7 days, after that samples removed from water and heated in oven at 150°C for 2 hours, finally samples will be weighing again and the values will be denoted by (W_f). The percentages of weight loss by water exposure or leaching were calculated from equation below.

$$\% \text{ Weight loss} = ((W_i - W_f) / W_i) * 100 \quad (4.2)$$

4.3.3. DTA-TG Analysis

DTA-TG test were performed by DTA HITACHI-STA 7300 device up to 600°C temperature with the heating rate of 7°/Min.

4.3.4. XRD Analysis

Rigaku ultra iv XRD device was used for X-Ray Diffraction analyses. An analysis ranges were 5 to 70 degree and analyze rate is 5°/minute.

4.3.5. SEM Analysis

SEM analyses were performed with Carl Zeiss Ultra Plus Gemini FESEM device. Samples were coated with gold to obtain conductivity before tests.

4.3.6. FTIR Analysis

Fourier Transform Infrared Spectroscopy (FTIR) analyses performed with Bruker Alpha device at transmittance mode between 400-4000 cm^{-1} .

PART 5

RESULTS AND DISCUSSION

5.1. APPEARANCE OF THE SAMPLES

All samples have a sufficient strength to handle, and sample preparation such as sanding the surface before strength tests were applied. The samples showed gradually change in color from the color of reference samples depending on the amounts of additives and type of additives (Figure 5.1). The samples of GGBFS additives showed changing in color toward green, while the samples of metakaolin additives showed brown color but the samples of waste glass additives showed changing toward white color, meanwhile the color of reference samples was yellowish. The change in color considered evidence that ensuring the occurrence of alkali activation reactions and impurities. The color change after drying process related to alkali activation process (in reference samples), but the change in color between series seems more related to type of the additives.

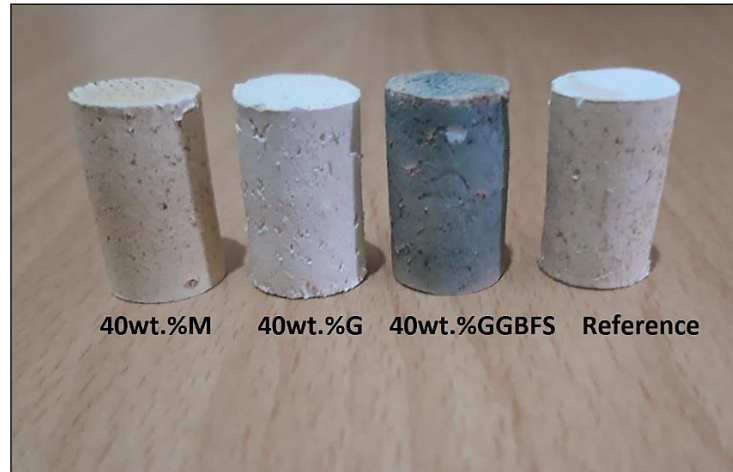


Figure 5.1. Appearance of the samples produced with different additives; M; Metakaolin, G; Waste glass powder and GGBFS; Ground granulated blast furnace slag.

5.2. COMPRESSIVE STRENGTH RESULTS

The compressive strength values of the samples are given in Figure 5.2. The compressive strength results present superior values in comparison with previous research [28,133,136,138,147] using un calcined kaolinite as a main source of aluminosilicate.

The series of GGBFS additives samples showed the highest compressive strength in addition ratio of 20wt.% GGBFS, it's reached 11.20 MPa, after which the strength was gradually decreased with increment in GGBFS additive. The lowest compressive strength obtained from 10wt.%GGBFS, namely 3.4 MPa, this value is somewhat close to the strength of the reference samples which haven't any additive. This closeness in compressive strength values between 10wt.%GGBFS and reference samples may be interpreted as; the 10wt.% of GGBFS is insufficient to supplement the reaction with sufficient reactive materials to improve alkali activation process, meanwhile the samples of 30 and 40wt.%GGBFS showed reduction in compressive strength from the values recorded at 20wt.%GGBFS. The reduction in values of 30 and 40wt.%GGBFS may be attributed to the presence of excessive amount of un reacted precursor which are formed when cation of activator solution consumed completely in the reaction by more reactive GGBFS.

The series of metakaolin additive samples exhibited gradually increases in compressive strength; the higher strength obtained among all samples was recorded for 30wt.%M samples in value of 14.00 MPa. The lower strength noticed in metakaolin additive samples was for 40wt.% and the value was 6.85 MPa, this value is approximately two times higher than value obtained from reference samples of 3.1 MPa, this is assuring the considerable effect of more reactive metakaolin that support the reactions, consequently, improving compressive strength. The dropping in compressive strength after the optimum value of 30wt.%, may attributed to the exhausted alkali cation in the reaction so the ratio of weak un-reacted phase will increases axiomatically originated from hydrated kaolin that is soft and have plastic nature.

Many researchers [149-155] admits that the molar ratio of $\text{SiO}_2/\text{Al}_2\text{O}_3$ have a great influence on the compressive strength. The optimal ratio of $\text{SiO}_2/\text{Al}_2\text{O}_3$ precursor different from materials to other depending reactivity of silica and alumina in each material [156-158]. Davidovits who study the effect of Si/Al ratio on alkali activated metakaolin, proposed the optimal $\text{SiO}_2/\text{Al}_2\text{O}_3$ ratio is between 3.5 to 4.5 [150]; meanwhile, Fletcher et al. reported the optimal ratio of $\text{SiO}_2/\text{Al}_2\text{O}_3$ ratio for metakaolin activated by NaOH is 16 [151]. For GGBFS additive samples, Panagiotopoulou et al. optimize $\text{SiO}_2/\text{Al}_2\text{O}_3$ ratio of GGBFS based alkali activation; they found the optimum ratio of $\text{SiO}_2/\text{Al}_2\text{O}_3$ is 3.5.[120]. Bakharev et al. report that the activation of GGBFS with water glass gave higher compressive strength [159], this result was confirmed by Shi who reports GGBFS activated by NaOH exhibited lower compressive strength than using water glass or sodium carbonates [65]. Consequently, the probability of getting better results from GGBFS additives still needs further investigation. Regarding to metakaolin, Pinto report that the activator mixture of NaOH and water glass produce higher compressive strength than using NaOH alone with metakaolin [160]. The different point of the samples produced in this study was that the samples formulation not including sodium silicate solution to support the hydrosodalite crystallization or supporting amorphous polysialate geopolymer by feeding the system with high viscosity sodium silicate. By this way a negative effect of low Si/Al molar ratio in compressive strength will going on, but it is turn into advantage in production; thus, the lack of sodium silicate solution in precursor was allow to bring into action of

rapid heat curing approach. Wang et al. report metakaolin gave high compressive strength with high concentrated activator [161]. Regarding to kaolinite, Slaty et al. optimizing the effect of NaOH % by kaolinite clay weight in presence of sand, they found the optimum ratio of NaOH was gain at 16% by weight of kaolinite clay in fixed water percentage of 22% by kaolinite clay weight [134]. The NaOH concentration of activator solution used in these experiments is somehow lower than activator used by Slaty et al. [134].

The series of glass additives samples, although it's showed slightly development in compressive strength along with waste glass additives addition but it's not possible to say that waste glass powder improving compressive strength significantly. In comparison with metakaolin and GGBFS additives samples, the lower compressive strength recorded for glass additive samples may attributed to the low reactivity of both kaolinite [28,147] and waste glass [162,163], so that, the fast production method will hinder the reaction between precursors and activator, and this opinion agree with Cheng who said the compressive strength of alkali activated glass would be improved if aging process were applied [164]. Furthermore, many researchers attributed the reduction in compressive strength of samples based waste glass additive to the high concentration of activator [165, 166], its believed high concentration activator may cause alkali ions agglomeration around waste glass particles and hindering reaction due to the restriction of ions movement in the structure [167],in the same context, there is another opinion attributed that to the raising of NaOH activator viscosity and destroying structure thus hindering geopolymerization reaction[168,169]. Likewise, according to Cercel et al. the low content of alumina in waste glass powder may have a negative role in reaction progression [162]. It's important to say, these compressive strength results are two times high than the result obtained by Bilondi et al. who studied the improvement of mechanical properties of clay soils by using rang of recycled glass powder (from 0% to 25%) under long curing periods (7, 28, 91 days) and temperature of 25°C and 70°C with NaOH activator solution varied from 1M to 8M [129]. Redden et al. got similar result to these we obtained when they try ternary mixture of 50% glass powder, 25% metakaolin and 25% GGBFS, this mixture activated by 4M of NaOH solution. They found using glass alone gave better compressive strength than using in a mixture at short curing periods [170]. As a summary, glass powder was not having

effective reactivity to behave like a precursor promoter but it seems waste glass powder behave like an ordinary inert filler due to its low reactivity in terms of compressive strength values (Figure 5.2).

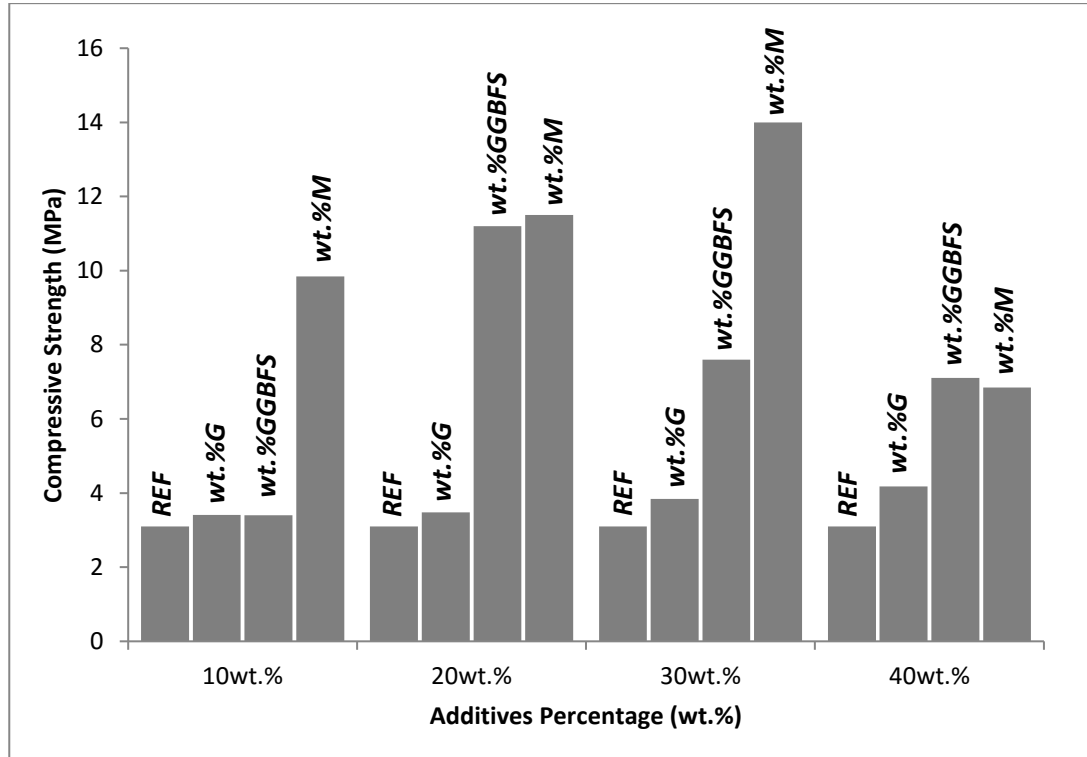


Figure 5.2. Compressive strength of the samples.

5.3. WATER RESISTANCE AND WATER ABSORPTION OF THE SAMPLES

In general, all samples did not show any cracks or disintegration even in water, and this result coming compatible with results of Heah et al. [132].

5.3.1. GGBFS Added Samples

The samples of GGBFS additives showed good result for weight loss percentage throughout 7 days of immersion. The percentages of weight loss were start increasing in a regular manner with time passed (from 1 day up to 7 days). The lower weight loss percentage was recorded for 20wt.%GGBFS samples after 1 day of soaking in water, the value was 2.27wt.%, and this good result appear agreed with compressive strength result of same samples, that's may have attributed to the high amounts of reacted

materials. The higher weight loss percentages were 4.95wt.%, its recorded for 10wt.%GGBFS samples after 7 days of soaking, whereas reference samples shown 7.05wt.% of weight loss after 7 days. The difference in weight loss percentage between reference samples and GGBFS additive samples are clearly proved the deeply influence of GGBFS additives on alkali activated kaolinite (Figure 5.3). The samples of GGBFS additives were the best between others two series in term of weight loss percentage in water, Yip et al. who studying the durability of kaolinite and GGBFS mixture, proposed that the presence of amorphous zeolitic phase and geopolymeric gel are responsible to the good durability and also they attributed the durability of ancient heritage to the presence of zeolitic materials [171], also, Campell et al. report: the good durability of ancient binder attributed to zeolitic structure formed [172].

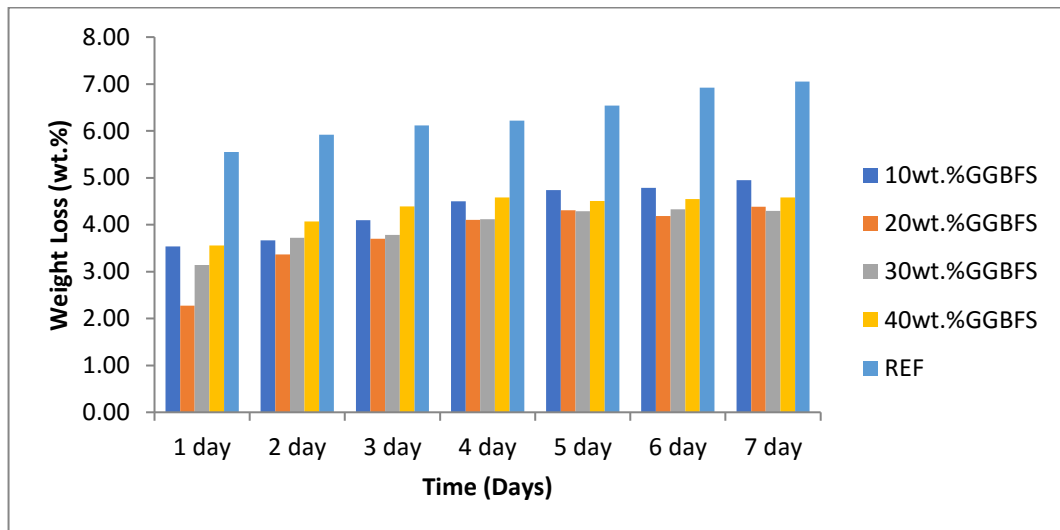


Figure 5.3. Weight loss (wt.%) of GGBFS added samples.

The samples of GGBFS additives showed a uniform influence to GGBFS addition in term of water absorption. Figure 5.4 showed inverse relationship between GGBFS addition and water absorption; consequently, water absorption percentages are gradually dropped from reference samples to 40wt.%GGBFS sample, that's leading to find the open porosity of samples decreasing with increasing GGBFS addition.

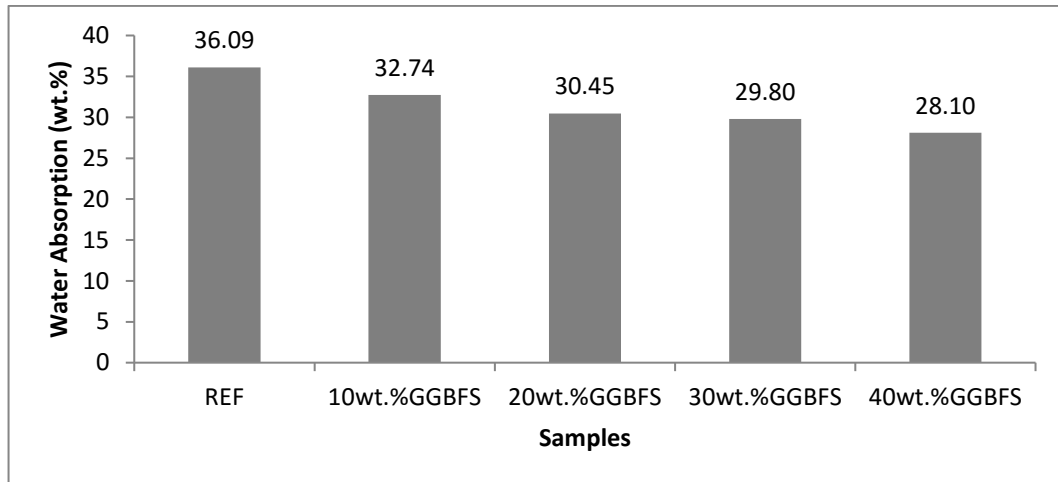


Figure 5.4. Water absorption (wt.%) of GGBFS added samples.

5.3.2. Metakaolin Added Samples

The samples of metakaolin additives have result near to those of GGBFS additive sample. In term of weight loss, Figure 5.5 showed that all samples' losses its weight in increasing manner with time, the lower weight loss percentage found after 1 day of soaking with 30wt.%M samples, the weight loss percentage was 2.78wt.%, these results are also supported by the result obtained from compressive strength test, whereas 30wt.%M samples present the higher compressive strength among all other metakaolin additive samples. The higher weight loss percentage was recorded at 7 days for samples of 10wt.%M in amount of 6.67wt.% which is lower than reference samples value of 7 days soaking which record 7.05wt.%. Although, the difference between maximum weight losses recorded at 10wt.%M and reference samples weight loss recorded at 7 days but the values are near to each other, that leading to believe the metakaolin additive effect may disappearing of over long periods, even for 30wt.%M samples.

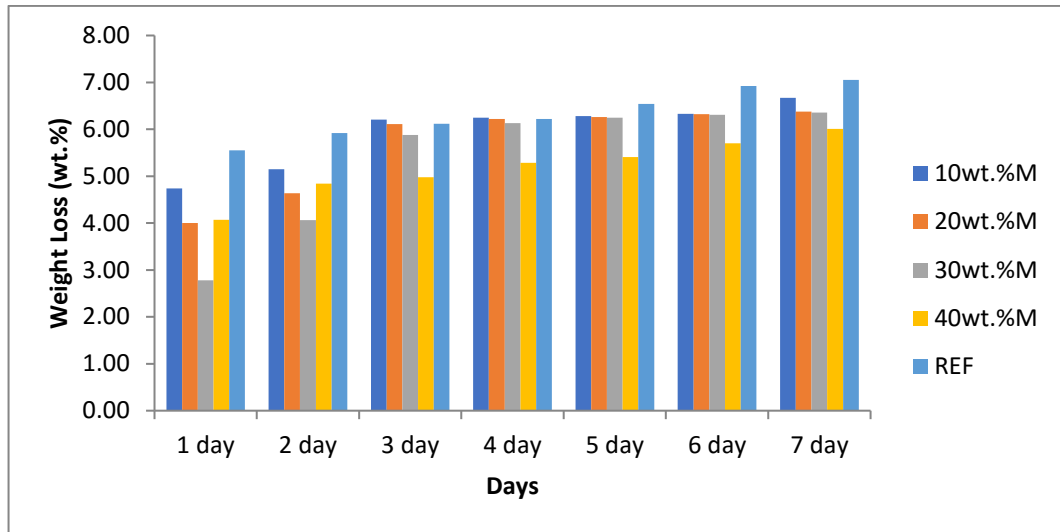


Figure 5.5. Weight loss (wt.%) of metakaolin added samples.

From Figure 5.6, The water absorption percentage of metakaolin additives samples present decreasing with metakaolin additive increasing. The higher water absorption recorded in 10M% samples, it was 34.60wt.%, but the lower value obtained from 40wt.%M samples in value of 25.00 (this was the best result among two other series), which is explaining the significant role of metakaolin in closing or reducing the open porosity of samples.

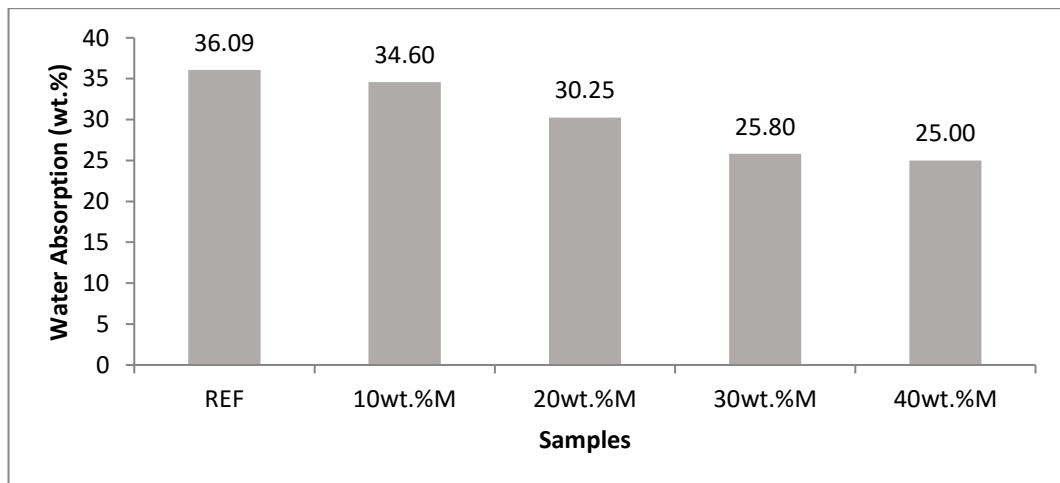


Figure 5.6. Water absorption (wt.%) of metakaolin added samples.

5.3.3. Waste Glass Powder Added Samples

The weight loss percentage of waste glass additives samples showed increasing in weight loss with time, but the relationship between weight loss and waste glass addition was clearly noticed (especially at 1 and 2 days of soaking in water), so, when waste glass additive increases the sample weight loss decreases (Figure 5.7). Although the samples of waste glass additive don't show good compressive strength result in comparison with reference samples but these samples exhibited good performance in term of water resistance. Similar to results previously obtained from GGBFS and metakaolin based additive samples, waste glass additives samples present decreasing in water adsorption ratios with increasing waste glass powder addition (Figure 5.8).

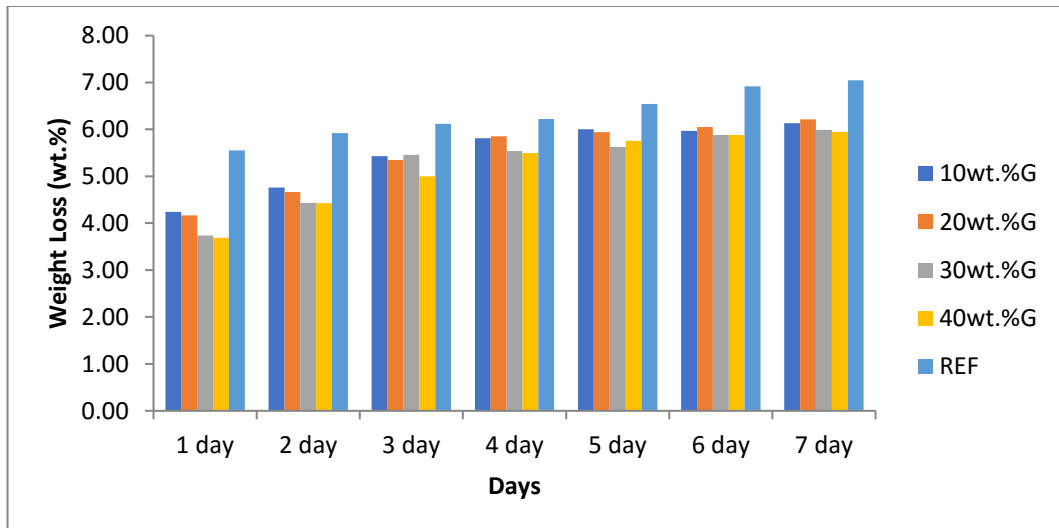


Figure 5.7. Weight loss (wt.%) of waste glass added samples.

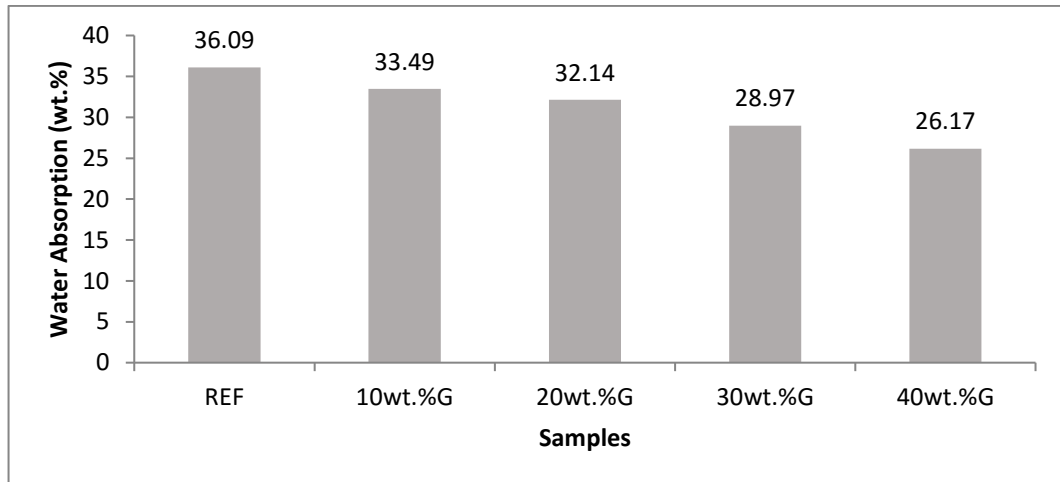


Figure 5.8. Water absorption (wt.%) of waste glass added samples.

5.4. XRD RESULTS

XRD analyses showed developing of new peaks after alkali activation process (Figure 5.9), these new peaks corresponded for hydrosodalite phases. The growing of these new peaks synchronized with degradation in intensities of kaolinite peaks, this was attributed to the dissolution of kaolinite as much as hydrosodalite formed and this observation agrees with certain scientific papers [35,173]. The low peaks intensities of hydrosodalite might be corresponded to the low reactivity of kaolinite which retain on its appearance even in further stages, and that may be interpreted as partial dissolution of kaolinite and consequently partials contribution in reaction, this justification was adopted by many publications [174,175-177].

The XRD peaks of samples with additives showed changing in the crystal structure into more amorphous structure in comparison with reference samples; this was observed by the widening of the peaks and the weakening of the intensity. Many researches confirmed the formation of NASH phases from metakaolin alkali activation [7,151,178-181] and CSH phase from GGBFS alkali activation [155,182-187], also, other researchers [170,188,189] confirmed the formation of sodium silicate gel when waste glass activated alone using NaOH but when activated with presence of Al-rich materials such as metakaolin a Na-Al-Si-zeolitic phase are formed. In spite of that, in these experiments, the additives materials did not show a formation of any other zeolite phase (when incorporated with kaolinite) differ from phases observed in reference

samples, that may interpret as; the additives materials were dissolve in NaOH solution leading to SiO₂, Al₂O₃ and CaO abundant in the mixture related to their chemistry. These solutions may be transforming to the amorphous geopolymeric structures with different chemical composition.

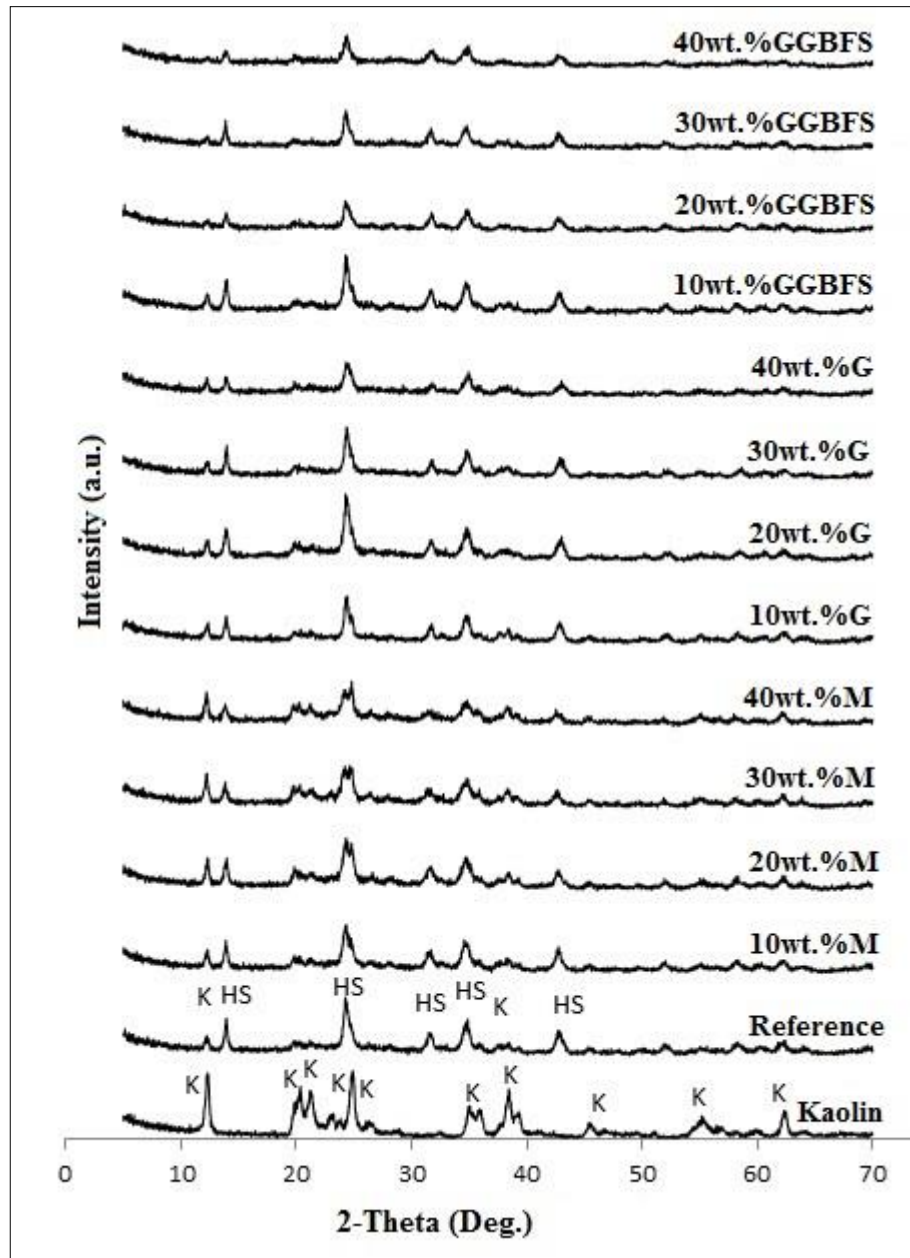


Figure 5.9. XRD pattern of the samples, K; kaolinite, HS; Hydrosodalite.

5.5. FTIR RESULTS

FT-IR spectrum of the precursors and samples are given in Figure 5.10. In accordance to Van Jaarsveld et al. the changes in absorption frequencies between kaolinite and geopolymer samples refer to the transformation of precursors through geopolymerization reaction [190]. Kaolinite FTIR graph shown certain absorbance bands at 3962 and 3620 cm^{-1} , which may be belonged to OH^- and H-O-H stretching vibration [133,136,191,192], and 1652 cm^{-1} band assigned for bending vibration of H_2O [139,191,193]. The absorption band at peak of 1116 cm^{-1} is assigned to symmetrical stretching of Si-O bond in tetrahedral of SiO_2 molecules in kaolinite crystal structure [192,194-198]. Many published papers attributed the peaks of 1028 cm^{-1} to stretching vibration of Si-O-Si [145,194,198,199], but others attributed this absorption peak to Si-O vibration [192,197]. There are three classifications related to 998 cm^{-1} peak; the first corresponded it Si-O-Si bond in plane vibration [145,198], the second assigned it as Si-O bond [145,199], the third sorted this peak to Si-O/Al-O bond alternatively [133]. The peaks of 907 cm^{-1} and 936 cm^{-1} were related to Al-OH bending vibration [139,145,192,197,198,200]. The peak of 791 cm^{-1} indicated to Al-OH [192,198] or to Si-O bonds [191,194]. The peak of 753 cm^{-1} referred to Si-O-Si bond stretching vibration [192] or Si-O-Al [197,201] or Al-OH [198]. The peak of 538 cm^{-1} recognized as Al-O-Si bond [190,192,201]. The peaks of 469 and 430 cm^{-1} attributed to Si-O bond [192,201].

After alkali activation process, 3620 and 3692 cm^{-1} peaks were disappeared that indicated to the evaporation of structural water in the samples. The peaks of 907 cm^{-1} noticed shifted over wave number position to 915 cm^{-1} in activated samples, which attributed to the alkalization process [133]. The main peaks around 950 to 998 it categorized to Si-O-T bond (symbol "T" refer to Al or Si) which indicates to the formation of 3D network of polysialate gel [27,191,193,202,203]. The emergence of new peaks with low absorption percentage located at 663, 706 and 734 cm^{-1} corresponded to Si-O-T which refer to the formation hydrosodalite [35,202,203]. The peaks of 530, 469 and 430 cm^{-1} continued appear in all activated samples, that was linked to the un reacted precursors which didn't contribute in alkali activation reaction [136,191,204].

FTIR graphs of waste glass added samples showed considerable peaks with glass additives in comparison with reference samples, Si-O-T peaks of 10%G appear more severe than those of reference samples, besides that, the peaks of 20, 30 and 40wt.%G seemed weaker than 10wt.%G.

Different from glass, FTIR graphs of GGBFS-additives sample showed clear and distinguished role for GGBFS, so that, the GGBFS act as second active resource of Si atoms in the mixture what increasing the formation of Si-O-T bonds. The peaks related to Si-O-T showed dropped back in 10wt.% GGBFS-additives samples but 20, 30 and 40wt.% GGBFS-additive samples showed elongation in Si-O-T peaks, this may attribute to high compressive strength results obtained from samples of 20wt.% GGBFS.

For metakaolin-additives samples, the role of Al_2O_3 was very clear especially in the widening of the main peak (Si-O-T bonds) which interpreted to the formation of Si-O-Al due to the abundant of active Al_2O_3 in metakaolin composition, the wider and higher peaks was observed at 10, 20 and 30wt.% metakaolin-additive samples and this what supported by the compressive strength results. The peaks of 3620 and 3692 cm^{-1} were still present in weak intensity at 10 and 20wt.%M spectrum. Generally, all samples showed retained bands corresponded to peaks appeared in precursor FTIR, especially at 469 and 430 cm^{-1} , these two peaks appeared in kaolinite so its refer to presence of the un reacted kaolinite.

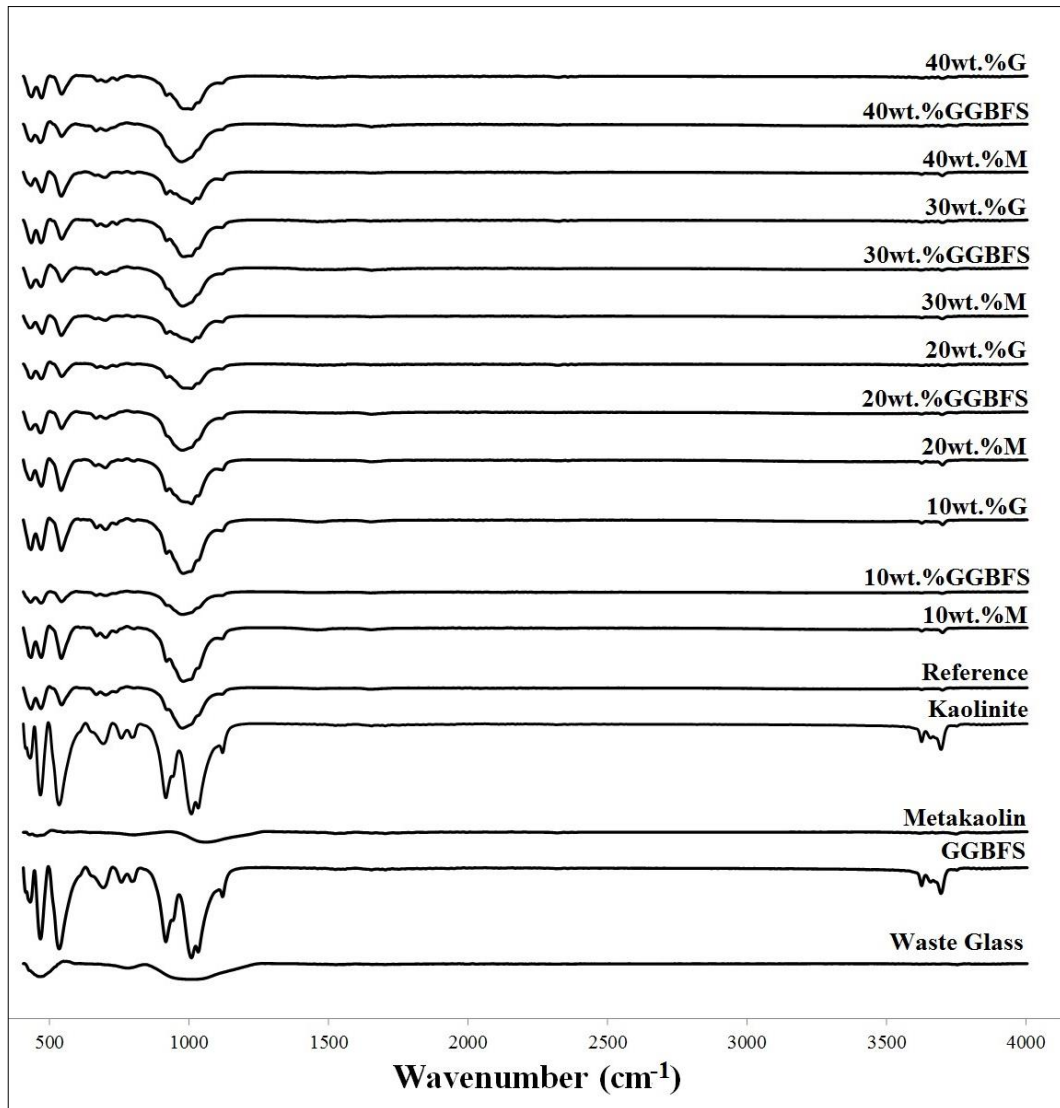


Figure 5.10. FTIR spectrum of the samples.

5.6. DTA-TG RESULTS

The DTA curves of the waste glass, metakaolin and GGBFS added samples are given in Figure 5.11, Figure 5.12 and Figure 5.13, respectively. The endothermic peaks present in kaolinite DTA curve at temperature around 500°C refer to dehydroxylation of kaolinite, at this stage the kaolinite's crystal structure were broken and forming amorphous metakaolin [205] (Figure 5.11). Additives including samples which didn't show violent dehydroxylation peaks may be related the consumed some of structural water into hydrosodalite formation. In metakaolin added samples dehydroxylation

peak was sharper than other additives including samples and that may attribute to re-hydration of metakaolin (Figure 5.12).

The TG curves of all produced samples showed two main stages of weight loss, the first before 300°C and the second at around 500°C, these two points of weight loss were justified by releasing of hydroxyl molecules. The weight loss under 300°C, it believed due to evaporation of zeolitic water, but the second drop in weight loss appears about 500°C is seemed to be matched with de-hydroxylation appear in DTA curves, that what refer to removing of structural hydroxyl molecules in remained kaolinite structure or hydroxides in alkali activated part.

All samples of waste glass additives showed lowest weight loss in comparison with reference samples, this result may attribute to the absence of structural hydroxyl molecules in the samples network and that what support the additives behavior of waste glass in kaolinite alkali activation process (Figure 5.14). Waste glass additives showed indirect relationship with TG%. Detected additives behavior was agreement with the results obtain from water absorption test (see Figure 5.8). Additives other than glass powder have complex thermogravimetric effects (Figure 5.15. and figure 5.16). Different parameters with different impacts compete in the curing process led to this result. These parameters can be listed as follows. The increase in unreacted kaolinite (due to the consummation of the alkali cations with more reactive additive) led to increased crystal water. The unreacted part of the additives will reduce both zeolitic and crystal water (in high addition ratios of additives). Conversion of additives to alkaline activated gels will increase zeolitic water. Increasing hydrosodalite transformation of kaolinite will reduce the proportion of crystal water. Finally, possible rehydration of metakaolin increases the crystal water in the mixture. Since the dominance of the mentioned variables will be affected by the additive type and the addition ratio, it was not possible to determine a trend with increasing addition ratio of metakaolin and GGBFS additives on thermogravimetry

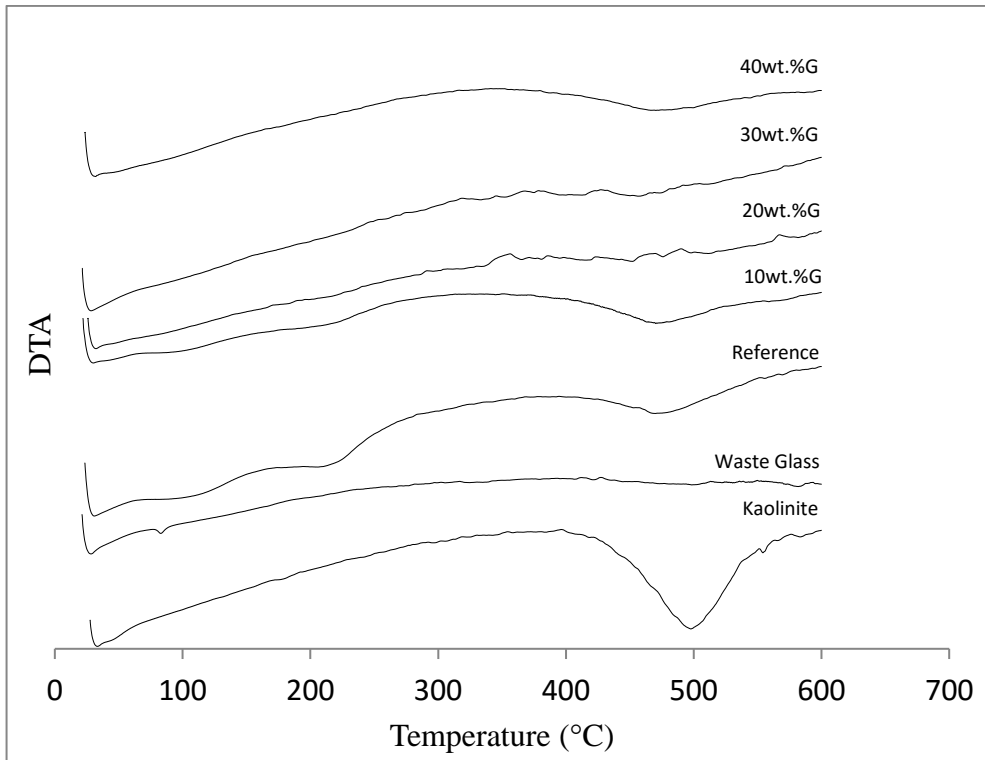


Figure 5.11. DTA curves of precursors, reference and waste glass powder added samples.

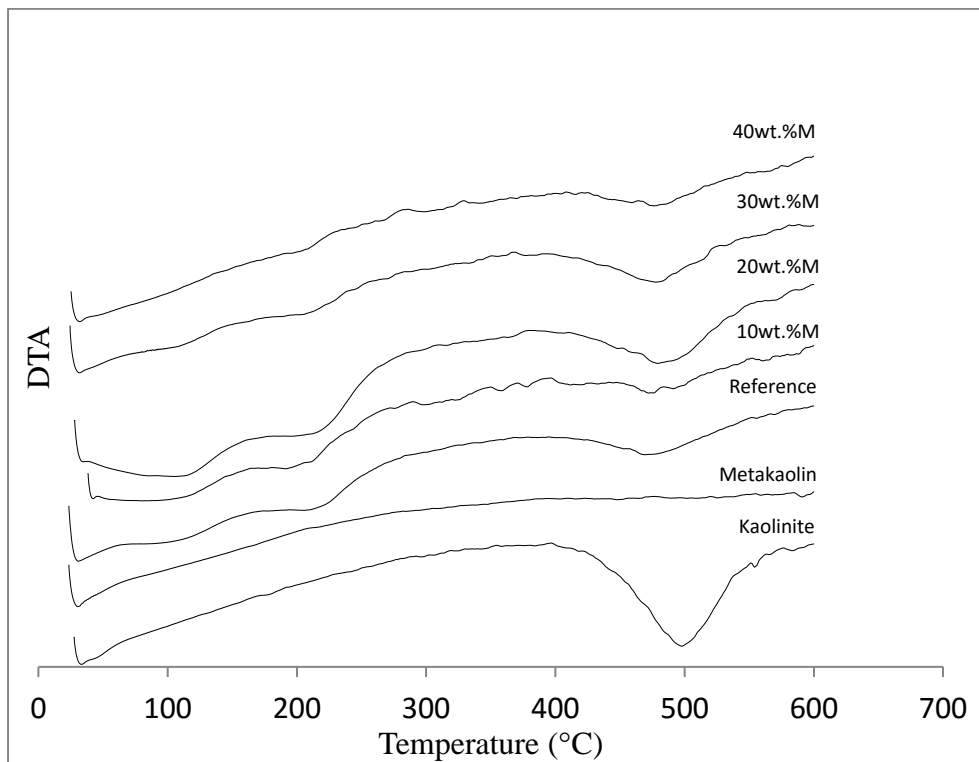


Figure 5.12. DTA curves of precursors, reference and metakaolin powder added samples.

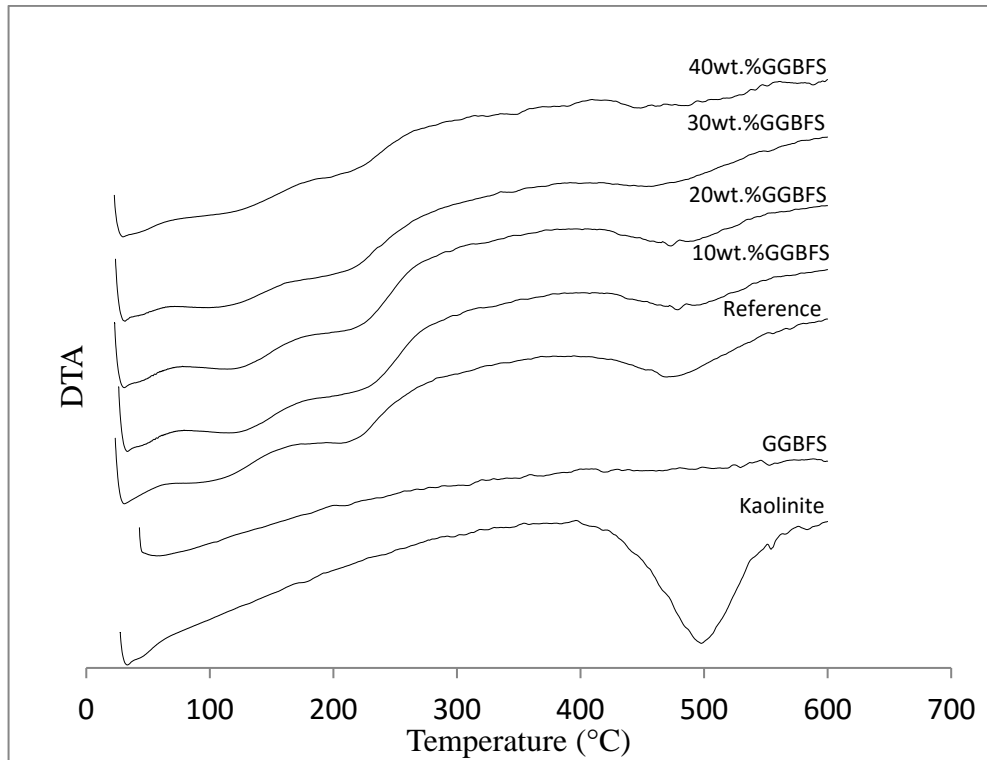


Figure 5.13. DTA curves of precursors, reference and GGBFS powder added samples.

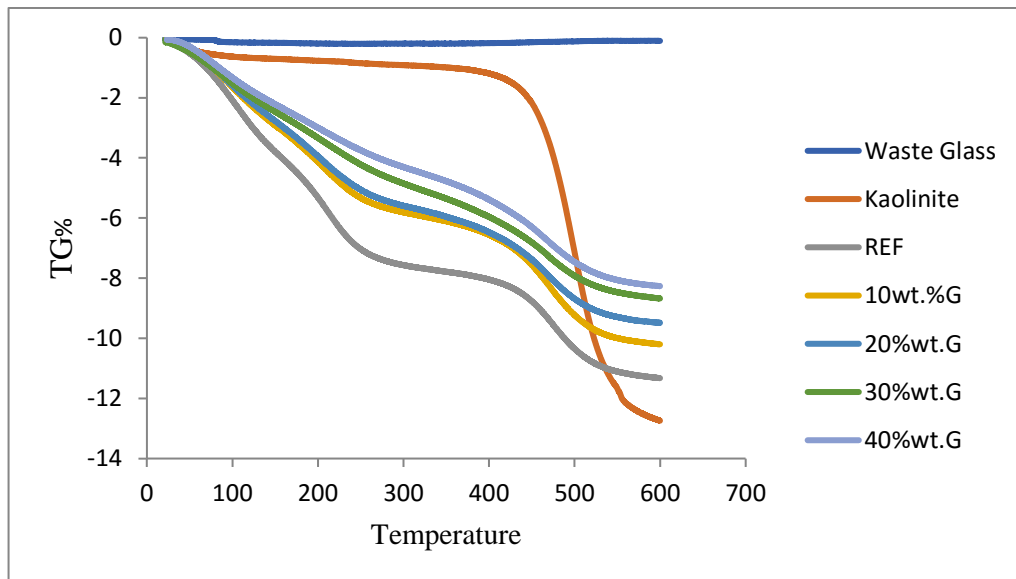


Figure 5.14. Thermogravimetry curves of precursors, reference and waste glass powder added samples.

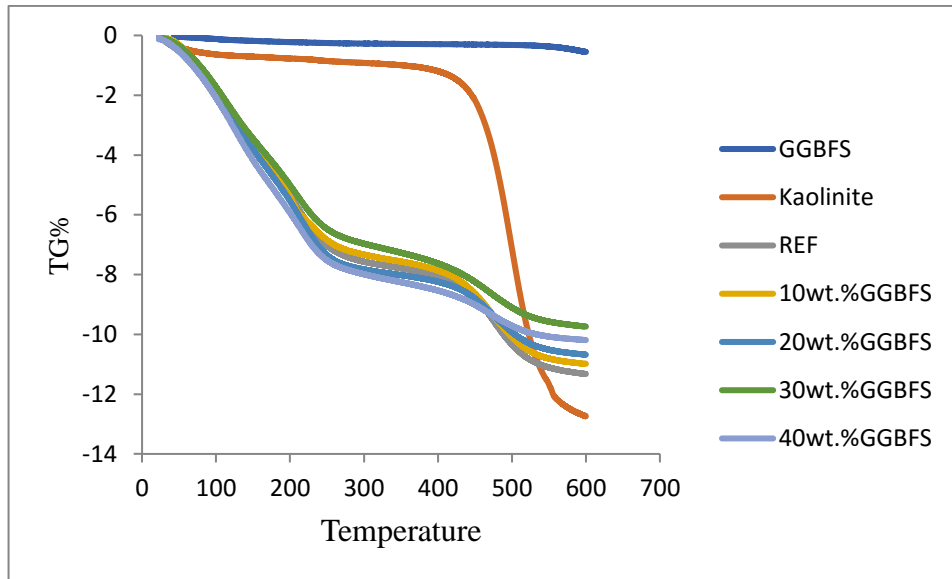


Figure 5.15. Thermogravimetry curves of precursors, reference and GGBFS powder added samples.

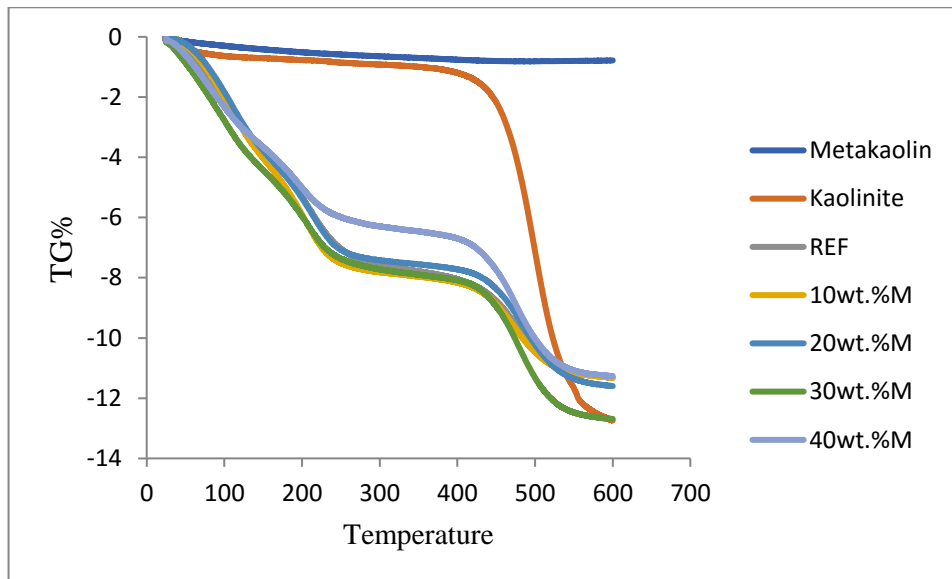


Figure 5.16. Thermogravimetry curves of precursors, reference and metakaolin powder added samples.

5.7. SEM RESULTS

All SEM photos showed evidence refer to hydrosodalite phase formation; these evidences were varied according to the additive's percentage and type of additive. In SEM photo the plate-like particles refer to kaolinite, but spheroidal-shape particle refers to hydrosodalite [35].

SEM photos of GGBFS added samples have good signs which assuring the occurrence of crystallization with crystal size better than crystals found in reference samples, thus the difference was noticeable between SEM photo of reference samples and additive samples, (Figure 5.17). 20wt.%GGBFS samples were the best among all GGBFS-additive samples in terms of hydrosodalite formation, (Figure 5.18), these results are matching with high compressive strength of 20w.%GGBFS (See Figure 5.2). The small size and irregular shape of hydrosodalite were may be attributed to the absence of hydrothermal conditions [206]. The sample of 10wt.%GGBFS didn't show significant change from reference samples, in other words, the role of 10wt.%GGBFS additive was so weak in improving activation reaction, (Figure 5.19), even the compressive strength data of reference samples were the nearest to the values obtained from 10wt.%GGBFS and that was a description for the light influence of 10wt.%GGBFS additives on samples. The role of GGBFS additives in hydrosodalite formation was clearly noticeable in the SEM photos of 20, 30 and 40wt.%GGBFS samples in comparison with reference sample. Although 30wt.%GGBFS and 40wt.%GGBFS samples showed crystal formation but un-reacted kaolinite stilled appear in SEM photo in high concentration, (Figure 5.20 and Figure 5.21).

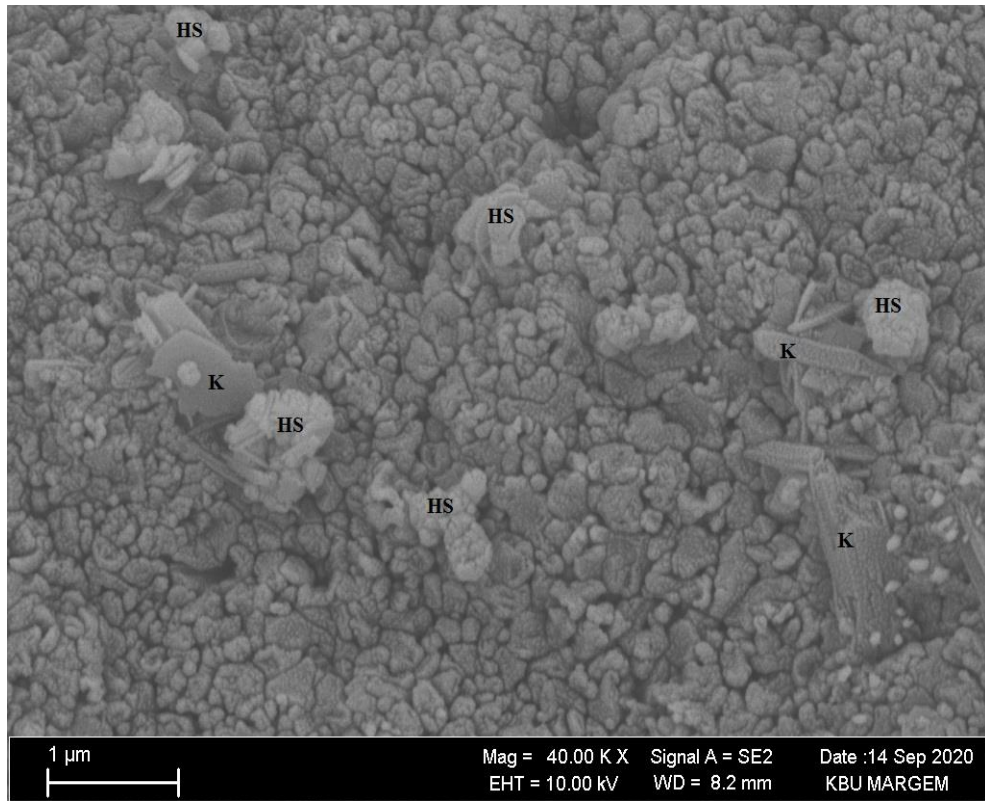


Figure 5.17. Microstructure reference sample. K; kaolinite, HS; Hydrosodalite.

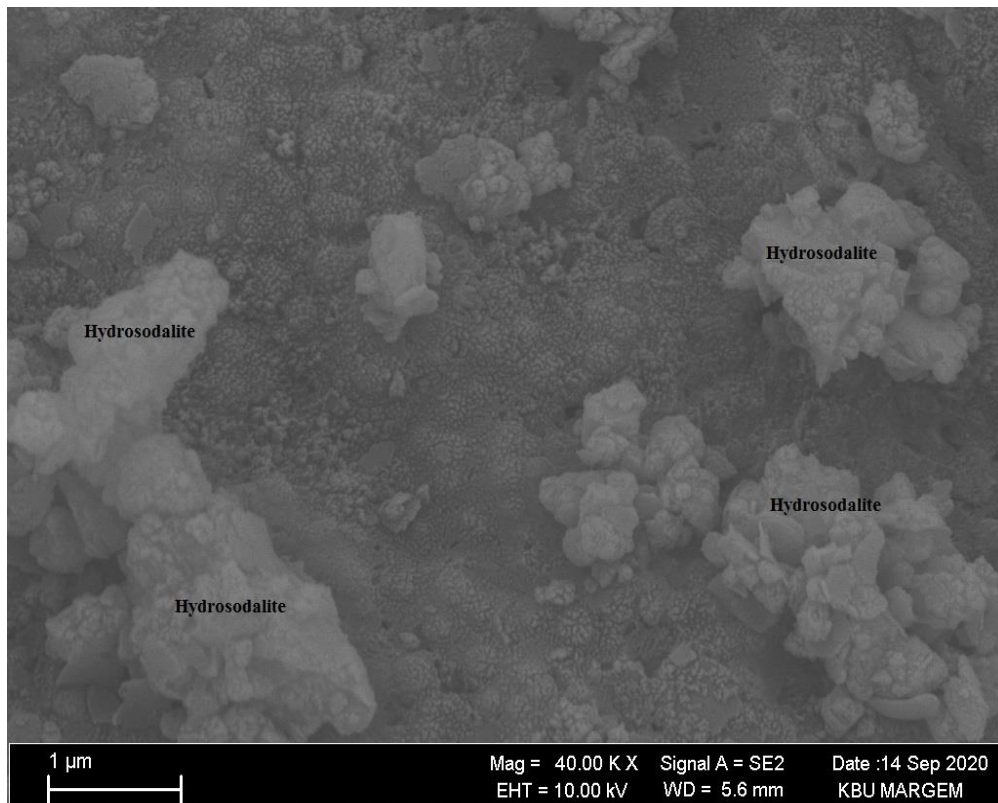
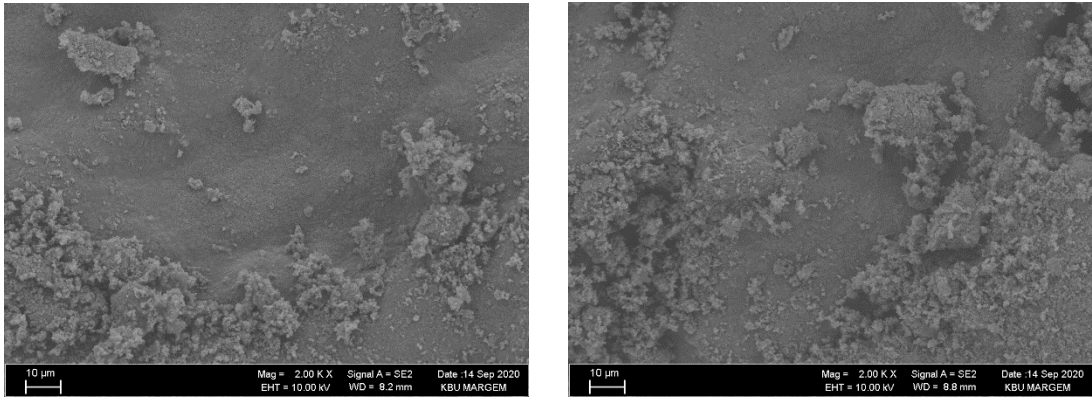


Figure 5.18. Microstructure of 20wt.% GGBFS added samples.



(a)

(b)

Figure 5.19. Microstructure of reference sample a) and 10wt.% GGBFS added samples b).

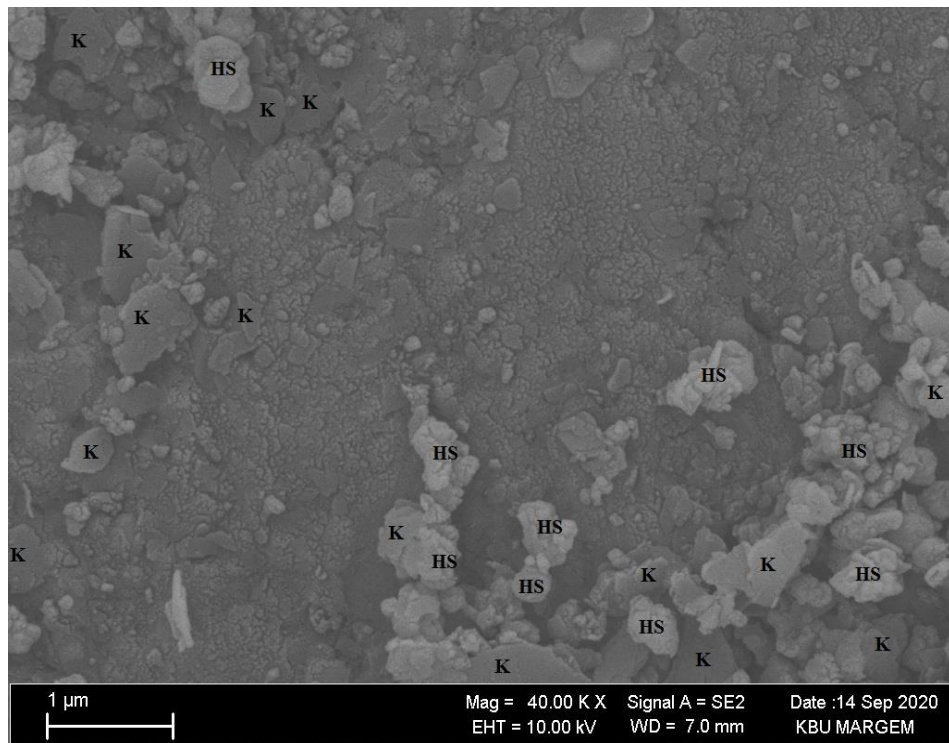


Figure 5.20. Microstructure of 30wt.% GGBFS added samples. K; kaolinite, HS; Hydrosodalite.

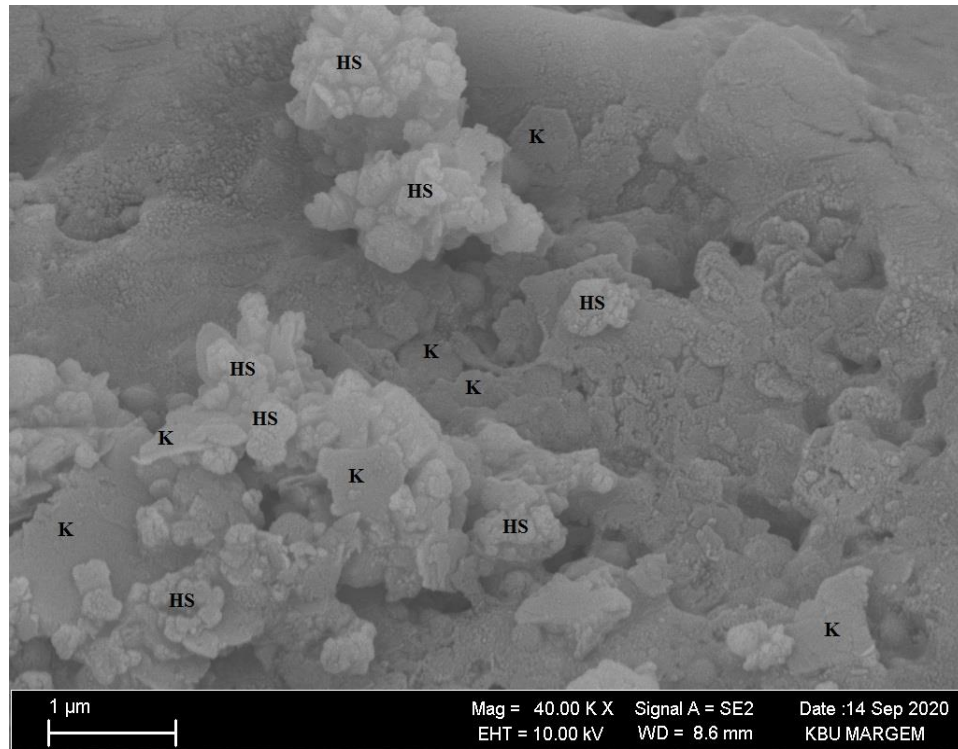


Figure 5.21. Microstructure of 40wt.%GGBFS added samples. K; kaolinite, HS; Hydrosodalite.

The SEM photo of the metakaolin added samples proved the creation of additional hydrosodalite crystal and that was occurred together with increasing compressive strength. The roles of metakaolin additives were highly impressive in all percentage, and the amount of hydrosodalite crystal formed was seems increased by increasing metakaolin percentage until 40wt.%M. The sample of 40wt.%M showed micro-crack existence in SEM photo, this is due to dry shrinkage and water evaporation, (Figure 5.22), and this may link to the dropping in compressive strength recorded at 40wt.%M, as well as the consumption of Na cation and hydroxyl molecules may also may be responsible. The samples of 30wt.%M showed the higher crystal size than other metakaolin-additive samples, (Figure5.23). All photos showed a presence of un reacted kaolinite alongside with hydrosodalite and this attributed to low kaolinite reactivity.



Figure 5.22. Microstructure of 40wt.% Metakaolin added samples.

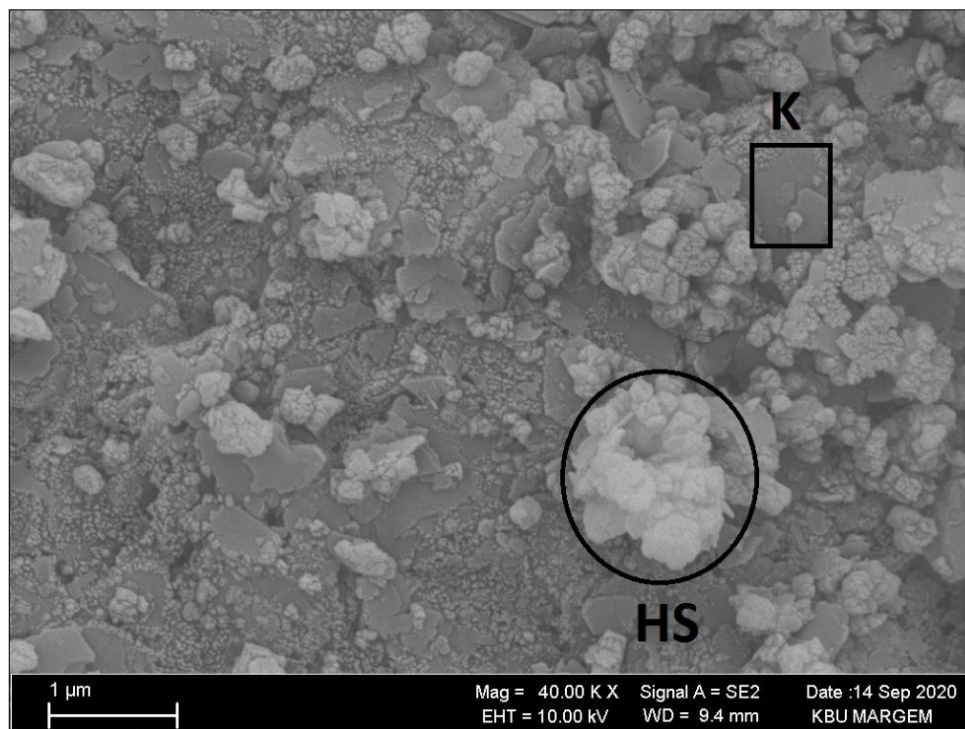
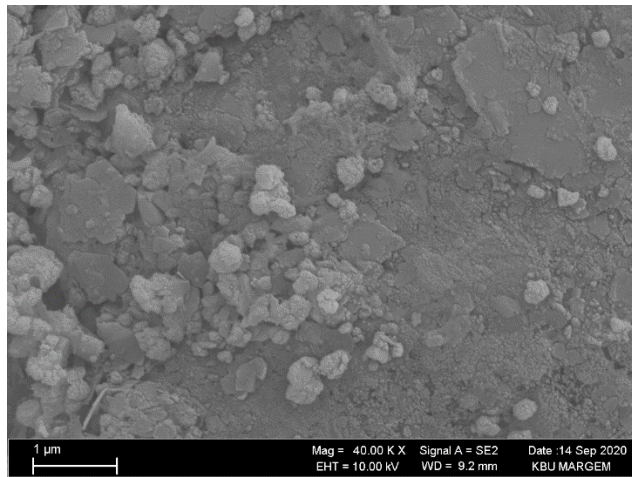
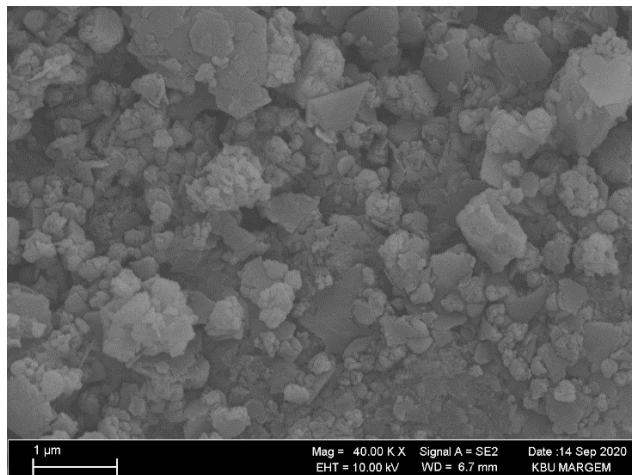


Figure 5.23. Microstructure of 30wt.% Metakaolin added samples. K ; kaolinite, HS ; Hydrosodalite.

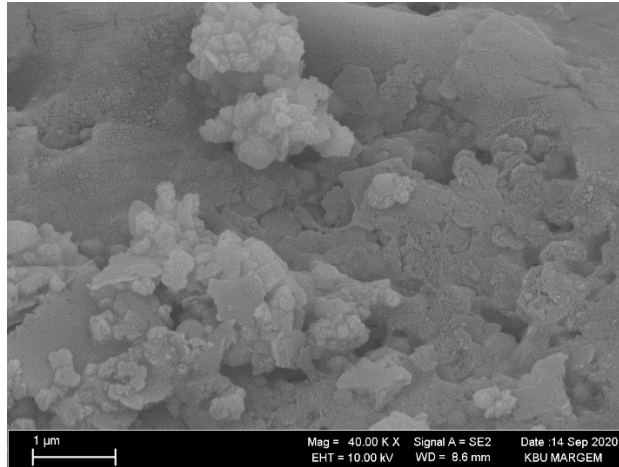
The result gotten from SEM showed; the samples of waste glass additives were the higher in having unreacted kaolinite among other series (Figure 5.24), also, SEM photos explained; the ratio of hydrosodalite structures increases with waste glass additives increased, (Figure 5.25 and Figure 5.26), however compressive strength result supports these findings. This result push us to say the un reacted kaolinite and low reactivity of waste glass weaken the reaction progression; in other words, the low reactivity of precursor restricts the spontaneous of reaction toward formation of aluminosilicate gel. Further, the low reactivity of glass and kaolinite doesn't permit to promote dissolution and polymerization reaction without longer curing periods.



(a)



(b)



(c)

Figure 5.24. Microstructure of 40wt.% waste glass a), 40% Metakaolin b) and 40%GGBFS c) added samples (continue).



Figure 5.25. Microstructure of 10wt.% waste glass added samples. K; kaolinite, HS ; Hydrosodalite.

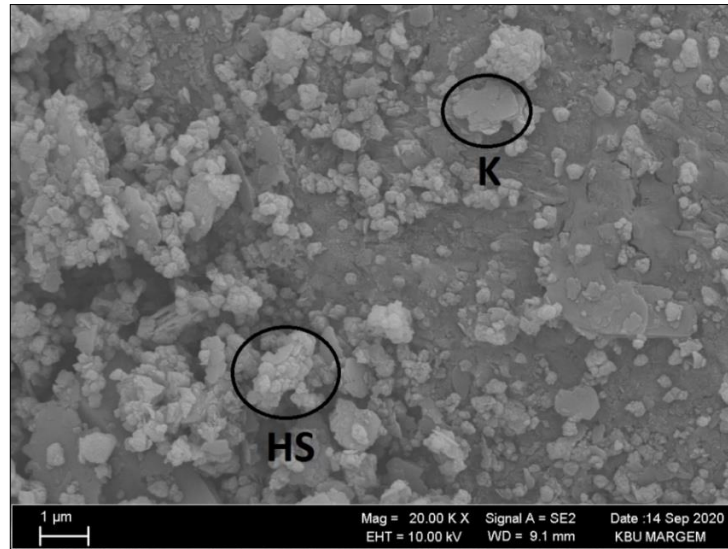


Figure 5.26. Microstructure of 30wt.% waste glass added samples. K ; kaolinite, HS ; Hydrosodalite.

Another important finding was observed in waste glass additives series, this observation was the micro-crack formation which may attributed to thermal shrinkage formed after structural water evaporation. Figure 5.27 and Figure 5.28 showed cracks noticed by SEM photo. This may be related to lack of plasticity at the samples during evaporation of water and may be the reason of low mechanical strength of the samples including waste glass powder in spite of their relatively good water resistant.

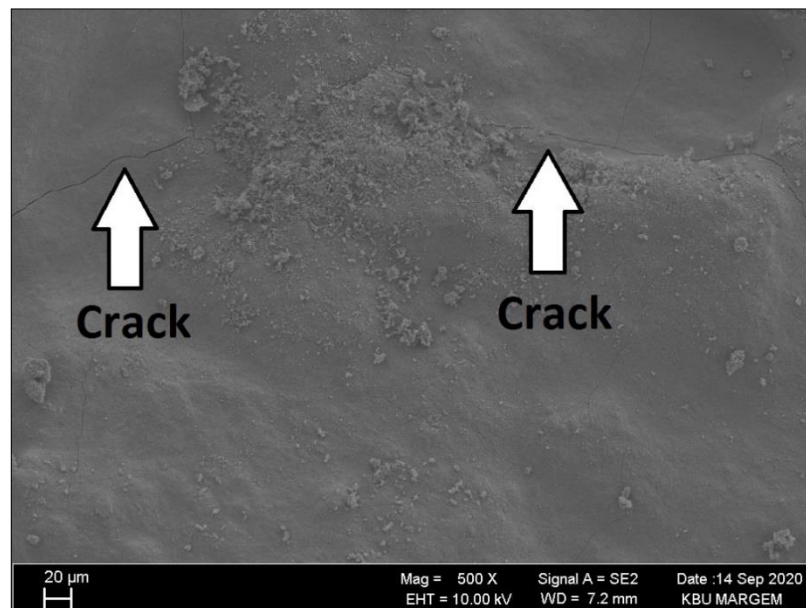


Figure 5.27. Microstructure of 20wt.% waste glass added samples.

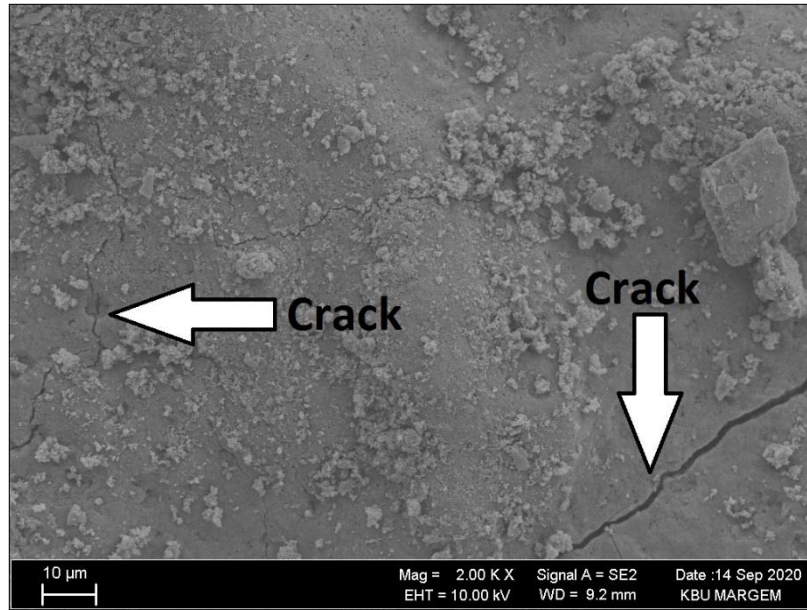


Figure 5.28. Microstructure of 40wt.% waste glass added samples.

PART 6

CONCLUSION AND SUGGESTION

In this work, kaolin based geopolymers (hydrosodalite based geopolymers) produced with the certain amount of additive (waste glass, GGBFS and metakaolin) and investigated in term of; compressive strength, water resistant, water absorption phase structure, bond structure and microstructure. Sample produced by rapid heat curing technique applied at 150°C that allows high productivity.

Regarding to compressive strength, the role of additives materials was perceptible and clear in comparison with reference samples. The samples of 30wt.%M showed highest compressive strength among other samples in value of 14.00 MPa. Compressive strength of the reference sample recorded as only 3.1 MPa. According to compressive strength result the optimum compositions in GGBFS additives samples and metakaolin additives samples were assigned to 20wt.%GGBFS and 30wt.%M, respectively. The samples of waste glass additives didn't show good result related to compressive strength test.

The result of water-resistant test present superiority for samples GGBFS additive, the sample of 20wt.%GGBFS showed lesser weight loss percentage (in value of 2.27wt.%), meanwhile, the higher weight loss percentage was assigned for reference samples (in value of 7.05wt.%). The water absorption percentage decreased gradually with additives increases.

XRD result confirms the formation of hydrosodalite phase in all produced samples. Also, some peaks appear were assigned to un reacted kaolinite due to low reactivity of kaolinite SEM results proved the formation of hydrosodalite crystals; on other side plate-like particles of un reacted kaolinite was observed too. The important finding

was observed is the formation of micro crack occurred due to thermal shrinkage causes by evaporation water content especially for glass powder added samples.

DTA-TG analysis showed endothermic peak at 500°C was attributed to dehydroxylation of kaolinite. Additives including samples didn't showed violent dehydroxylation peaks due to consumed most of structural water in reaction. TG curves showed weight loss related to zeolitic water and dehydroxylation for all samples. FTIR analysis supported a variation in intensities of peaks belonged to aluminosilicate bonds between reference and additives samples.

In general, the composition with 20wt%GGBFS and 30wt.%M were the optimum among other composition, so it's suitable to employ as low-cost construction materials and green production method that doesn't involved high energy consuming and huge tone of gases released because it's easy to reach 150°C by primitive and simple ways worldwide. It's important to mention that filler materials should be used for mass production in order to remove micro-crack formation through drying process for bigger products. There are needs for new studies investigating this binder with aggregates to manufacture various building materials.

REFERENCE

1. Davidovits, J., "Soft Mineralogy and Geopolymers", *Geopolymer 88 International Conference*, France, 19-23 (1988).
2. Živica, V., Palou, M. T., and Križma, M., "Geopolymer Cements and Their Properties: A Review", *Building Research Journal*, 61(2):85-100 (2015).
3. Mohsen, Q., and Mostafa, N., "Investigating the Possibility of Utilising Low Kaolinitic Clays in Production of Geopolymer Bricks", *Ceramics Silikaty*, 54(2): 160-168 (2010).
4. Davidovits, J., "Geopolymers: Ceramic-Like Inorganic Polymers", *Journal of Ceramic Science and Technology*, 8:335-350 (2017).
5. Davidovits, J., "Geopolymers Chemistry and Applications 2nd Ed.", *Institut Geopolymere*, Saint-Quentin, France, 1-570 (2008).
6. Roy, D., "Alkali-Activated Cements Opportunities and Challenges", *Cement and Concrete Research*, 29(2):249-254 (1999).
7. Pacheco-Torgal, F., Castro-Gomes, J. and Jalali, S., "Alkali-Activated Binders: A Review: Part 1. Historical Background, Terminology, Reaction Mechanisms and Hydration Products", *Construction and Building Materials*, 22:1305-1314 (2008).
8. Davidovits J., "Environmentally Driven Geopolymer Cement Applications", *Geopolymer 2002 3rd International Conference: Turning Potential into Profit*, Melbourne, 1-9 (2002).
9. Provis, J., Duxson, P., and Van Deventer, J., "Geopolymer Technology and The Search for A Low-CO₂ Alternative to Concrete", *2007 AIChE Annual Meeting. American Institute of Chemical Engineers*, United States, 1-13 (2007).
10. Palomo, A., Macias, A., Blanco-Varela, T., and Puertas, F., "Physical, Chemical and Mechanical Characterization of Geopolymers", *9th International Congress on The Chemical of Cement*, India, 5:505-511 (1992).
11. Aziz, H., Al Bakri, A., Cheng, H., Yun Ming, L., Hussin, K., and Azimi, A., "A Review on Mechanical Properties of Geopolymer Composites for High Temperature Application", *Key Engineering Materials*, 660:34-38 (2015).

12. Davidovits, J., "Properties of Geopolymers Cements", *First International Conference on Alkaline Cements and Concretes*, Ukraine, 1:131-149 (1994).
13. Bell, J., Gordon, M. and Kriven, W., "Use of Geopolymeric Cements as A Refractory Adhesive for Metal and Ceramic Joins", *Ceramic Engineering and Science Proceedings*, 26(3):407-413 (2005).
14. Comrie, D., and Davidovits, J., "Long Term Durability of Hazardous Toxic and Nuclear Waste Disposals", *1st European Conference on Soft Mineralogy*, France, 1:125-134 (1988).
15. Rangan, B., Hardjito, D., Wallah, S., and Sumajouw, M., "Studies on Fly Ash-Based Geopolymer Concrete", *Proceedings of The World Congress Geopolymer*, France, 28:133-137 (2005).
16. Xu, H., and Van Deventer, J. S. J., "The Geopolymerisation of Alumino-Silicate Minerals", *International Journal of Mineral Processing*, 59(3):247-266 (2000).
17. Litvinova, L., "Synthetic Polymers | Thin-Layer (Planar) Chromatography" Reference Module in Chemistry, Molecular Sciences and Chemical Engineering, Editors: Ian D. Wilson, *Academic Press*, US, 4348-4354 (2000).
18. Davidovits, J., "Geopolymers: Inorganic Polymeric New Materials", *Journal of Thermal Analysis and Calorimetry*, 37(8):1633-1656 (1991).
19. Garcia-Lodeiro, I., Palomo, A., and Fernandez-Jimenez, A., "2- An Overview of The Chemistry of Alkali-Activated Cement-Based Binders", Handbook of Alkali-Activated Cements, Mortars and Concretes, *Woodhead Publishing*, US, 19-47 (2015).
20. Davidovits, J., "Mineral Polymers and Methods of Making Them", *US Patent No 4472 1993*, 1-10 (1982).
21. Xu, H., and Van Deventer, J.S.J., "The Geopolymerisation of Aluminosilicate Minerals", *International Journal of Mineral Processing*, 59(3):247-266 (2000).
22. Kobayashi, T., "Applied Environmental Materials Science for Sustainability", *Igi Global*, USA, 168-222 (2016).
23. Schroeder, P., and Erickson, G., "Kaolin: From Ancient Porcelains to Nanocomposites", *Elements*, 10:177-182 (2014).
24. Varga, G., "The Structure of Kaolinite and Metakaolinite", *Epitoanyag*, 59(1): 6-9 (2007).
25. Cheng, H., Hazlinda, K., Al-Bakri, A., Luqman, M., Nizar, K., and Liew, M., "Potential Application of Kaolin Without Calcine as Greener Concrete: A Review", *Australian Journal of Basic and Applied Sciences*, 5:1026-1035 (2011).

26. Khalifa, Z., Cizer, Ö., Pontikes, Y., Heath, A., Patureau, P., Bernal, A., and Marsh, T., “Advances in Alkali-Activation of Clay Minerals”, *Cement and Concrete Research*, 132(106050):1-28 (2020).
27. San Cristóbal, G., Castelló, R., Luengo, M., and Vizcayno, C., “Zeolites Prepared from Calcined and Mechanically Modified Kaolins: A Comparative Study”, *Applied Clay Science*, 49(3):239-246 (2010).
28. Heah, Y., Kamarudin, H., Al Bakri Abdullah, M., Binhussain, M., Musa, L., Khairul Nizar, I., and Liew, M., “Effect of Mechanical Activation on Kaolin-Based Geopolymers”, *Advanced Materials Research, Trans Tech Publications Ltd.*, (479-481):357-361 (2012).
29. San Cristóbal, A., Castelló, R., Luengo, M., and Vizcayno, C., “Acid Activation of Mechanically and Thermally Modified Kaolin’s”, *Materials Research Bulletin*, 44(11):2103-2111 (2009).
30. Pacheco-Torgal, F., Castro-Gomes, J., and Jalali, S., “Alkali-Activated Binders: A Review. Part 2. About Materials and Binders Manufacture”, *Construction and Building Materials*, 22(7):1315-1322 (2008).
31. Luukkonen, T., Abdollahnejad, Z., Yliniemi, J., Kinnunen, P., and Illikainen, M. “One-Part Alkali-Activated Materials: A Review”, *Cement and Concrete Research*, 103:21-34 (2018).
32. Duxson, P., Provis, L., Lukey, C., and Van Deventer, S., “The Role of Inorganic Polymer Technology in The Development Of ‘Green Concrete’”, *Cement and Concrete Research*, 37(12):1590-1597 (2007).
33. Davidovits, R., Plelegris, C., and Davidovits, J., “Standardized Method in Testing Commercial Metakaolins For Geopolymer Formulations”, *Geopolymer Institute Library*, Saint-Quentin, France, 1-8 (2019).
34. Heah, C., Hussin, K., Al Bakri Abdullah, M., Bnhussain, M., Musa, L., Khairul Nizar, I., and Liew, M., “Strength and Microstructural Properties of Mechanically-Activated Kaolin Geopolymers”, *Advanced Materials Research, Trans Tech Publications Ltd.*, 626:926-930 (2013).
35. Marsh, A., Heath, A., Patureau, P., Evernden, M., and Walker, P., “A Mild Conditions Synthesis Route to Produce Hydrosodalite From Kaolinite, Compatible with Extrusion Processing”, *Microporous and Mesoporous Materials*, 264:125-132 (2018).
36. Esaifan, M., Rahier, H., Barhoum, A., Khoury, H., Hourani, M., and Wastiels, J., “Development of Inorganic Polymer by Alkali-Activation of Untreated Kaolinitic Clay: Reaction Stoichiometry, Strength and Dimensional Stability”, *Construction and Building Materials*, 9:251-259 (2015).

37. Davidovits, J., "Geopolymer Chemistry and Applications 2nd Ed.", *Institute Geopolymere*, Saint Quentin, France, 1-674 (2008).
38. Provis, L., "Alkali-Activated Materials", *Cement and Concrete Research*, 114:40-48 (2018).
39. Kuehl, H., "Slag Cement and Process of Making the Same", *US Patent, 900.939*, 1-2 (1908).
40. Purdon, O., "The Action of Alkalis on Blast-Furnace Slag". *Journal of The Society of Chemical Industry*, 59(9):191-202 (1940).
41. Eren, E., Moroydorderun, E., Piskin, S., "Investigation of The Effects of Boric Acid and Boric Acid Waste on The Alkaline Activation of Blast Furnace Slag", *Sigma Journal of Engineering and Natural Sciences*, 36(2):475-486 (2018).
42. Glukhowsky, D., "Soil Silicates", *Gostroiizdat Publishers*, Kiev (1959).
43. Malinowski, R., "Concretes and Mortars in Ancient Aqueducts", *Concrete International*, 1(1):66-76 (1979).
44. Contenson H, Courtois L. "A Propos des Vases De Chaux: Recherchessurleur Fabrication Et Leurorigine", *Paleorient*, 5:177-82 (1979).
45. Périnet, G., De Contenson, H., and Courtois, L., "Mineralogie-Étudeminéralogique De Vaiselles Blanches Neolithiques De Ras-Shamra Et Tell Ramad (Syrie)", *Comptesrendus De l'Académie Des Sciences*, 4:143-146 (1980).
46. Davidovits, J., "Ancient and Modern Concretes: What Is the Real Difference". *Concrete International*, 9:12-23 (1987).
47. Davidovits, J. and Courtois, A., "DTA Detection of Intra-Ceramic Geopolymeric Setting in Archaeological Ceramics and Mortars", *Abstracts of Papers 21st Symposium on Archaeometry*, New York, 1- 22 (1981).
48. Davidovits, J., "Geopolymeric Reactions in Archaeological Cements and In Modern Blended Cements", First *European Conference on Soft Mineralogy, Geopolymer 88*, 1:93-106 (1988)
49. Langton, C., and Roy, M., "Longevity of Borehole and Shaft Sealing Materials: Characterization of Ancient Cement-Based Building Materials", *MRS Online Proceedings Library Archive*, 26: 543-549 (1983).
50. Malone, G., Randall, A., Kirkpatrick, T., "Potential for Use of Alkali-Activated Alumino-Silicate Binders in Military Applications", *Report WES/MP/GL-85-15, Department of The US Army, Waterways Experiment Station*, USA, 1-44 (1985).

51. Davidovits, J., Sawyer, L., “Early High-Strength Mineral Polymer”, *U.S. Patent 4,509,985*, 1-13 (1985).
52. Krivenko, P., “Synthesis of Binders with Special Properties in A System $\text{Me}_2\text{O}-\text{MeO}-\text{Me}_2\text{O}_3-\text{SiO}_2-\text{H}_2\text{O}$ ”, *Ph.D. Thesis, Civil Engineering Institute*, Kiev, (1986).
53. Krivenko, P. “Why Alkaline Activation-60 Years of The Theory and Practice of Alkali-Activated Materials”, *Journal of Ceramic Science and Technology*, 8(3):323-333 (2017).
54. Kaushal, S., Roy, M., and Licastro H., “Heat of Hydration and Characterization of Reaction Products of Adiabatically Cured Fly Ash and Slag Mixtures”, *MRS Online Proceedings Library Archive*, 136-187 (1988).
55. Deja, J. and Malolepszy, J., “Resistance of Alkali-Activated Slag Mortars to Chloride Solution”, *Special Publication*, 114: 1547-1564 (1989).
56. Roy, M., and Langton, A., “Studies of Ancient Concrete as Analog’s of Cementitious Sealing Materials for A Repository in Tuff”, No. LA-11527-MS, *Los Alamos National Lab.*, USA, 1-101 (1989).
57. Majumbar, J., Singh, B. and Edmonds, N., “Hydration of Mixtures of C12A7 And Granulated Blast Furnace Slag”, *Cement and Concrete Research*, 19(6): 848-856 (1989).
58. Talling, B. and Brandstetr, J., “Present State and Future of Alkali-Activated Slag Concretes”, *Special Publication*, 114:1519-1546 (1989).
59. Roy, D., Silsbee, M., and Wolfe-Confer, D., “New Rapid Setting Alkali Activated Cement Compositions”, *MRS Proceedings*, 179:203-218 (1990).
60. Wu, X., Jiang, W. and Roy, D.M., “Early Activation and Properties of Slag Cement”, *Cement and Concrete Research*, 20(6):961-974 (1990).
61. Roy, D., and Silsbee, M., “Alkali Activated Cementitious Materials: An Overview”, *MRS Proceedings*, 245:153-164 (1991).
62. Palomo, A., and Glasser, P., “Chemically-Bonded Cementitious Materials Based on Metakaolin”, *British Ceramic. Transactions and Journal*, 91(4):107-112 (1992).
63. Glukhovskiy, D., “Ancient, Modern and Future Concretes”, *First International Conference on Alkaline Cements and Concretes*, Ukraine, 1-9 (1994).
64. Wang, D. and Scrivener, L., “Hydration Products of Alkali Activated Slag Cement”, *Cement and Concrete Research*, 25(3):561-571 (1995).

65. Shi, C., “Strength, Pore Structure and Permeability of Alkali-Activated Slag Mortars”, *Cement and Concrete Research*, 26(12):1789-1799 (1996).
66. Fernández-Jiménez, A., and Puertas, F., “Alkali-Activated Slag Cements: Kinetic Studies”, *Cement and Concrete Research*, 27(3):359-368 (1997).
67. Katz, A., “Microscopic Study of Alkali-Activated Fly Ash”, *Cement and Concrete Research*, 28(2):197-208 (1998).
68. Palomo, A., Grutzeck, W., and Blanco, T., “Alkali-Activated Fly Ashes: A Cement for The Future”, *Cement and Concrete Research*, 29(8):1323-1329 (1999).
69. Gong, C. and Yang, N., “Effect of Phosphate on The Hydration of Alkali-Activated Red Mud–Slag Cementitious Material”, *Cement and Concrete Research*, 30(7):1013-1016 (2000).
70. Krivenko, P., and Kovalchuk, Y., “Heat-Resistant Fly Ash Based Geocements”, *International Conference “Geopolymers”*, Australia, 1-10 (2002).
71. Provis, L., “Alkali-Activated Materials”, *Cement and Concrete Research*, 114:40-48 (2018).
72. Bernal, A., Provis, L., Fernández-Jiménez, A., Krivenko, V., Kavalerova, E., Palacios, M. and Shi, C., “Binder Chemistry-High-Calcium Alkali-Activated Materials”, Alkali Activated Materials, Editors; Provis, L., and Van Deventer, J., *Springer*, Dordrecht, 59-91 (2014).
73. Glukhovskiy, D., Rostovskaja, S., and Rumyna, V., “High Strength Slag-Alkaline Cements”, *7th International Congress on The Chemistry of Cement*, 3:164-168 (1980).
74. Davidovits, J., “Geopolymer Chemistry and Properties”, *“Geopolymer 88”*, Saint-Quentin, France, 88(1):25-48 (1988).
75. Van Jaarsveld, S., Van Deventer, J., and Lorenzen, L., “Factors Affecting the Immobilization of Metals in Geopolymerized Fly Ash”, *Metallurgical and Materials Transactions B*, 29(1):283-291 (1998).
76. Fernández, G., “Activación Alcalina De Metacaolín Desarrollo De Nuevos Materiales Cementantes”, *Ph.D. Thesis, Universidad Autónoma De Madrid*, Spain (1998).
77. Criado, M., Palomo, A. and Fernández-Jiménez, A., “Alkali Activation of Fly Ashes. Part 1: Effect of Curing Conditions on The Carbonation of The Reaction Products”, *Fuel*, 84(16):2048-20540 (2005).

78. Provis, L., and Van Deventer, S., “Geopolymerisation Kinetics. 1. In Situ Energy-Dispersive X-Ray Diffractometry”, *Chemical Engineering Science*, 62(9):2309-2317 (2007).
79. Provis, L., Duxson, P., Van Deventer, J., and Lukey, C., “The Role of Mathematical Modelling and Gel Chemistry in Advancing Geopolymer Technology”, *Chemical Engineering Research and Design*, 83(7):853-860 (2005).
80. Provis, L., “Geopolymers and Other Alkali Activated Materials: Why, How, and What?”, *Materials and Structures*, 47(1-2):11-25 (2014).
81. Gamage, N., Liyanage, K., Fragomeni, S., and Setunge, S., “Overview of Different Types of Fly Ash and Their Use as A Building and Construction Material”, *International Conference of Structural Engineering, Construction and Management*, Sri Lanka :1-9 (2011).
82. Provis, J., and Van Deventer, J., “Alkali Activated Materials: State-Of-The-Art Report, RILEM TC 224-AAM”, *Springer Science and Business Media*, New York: 1-387 (2013).
83. Bakharev, T., “Geopolymeric Materials Prepared Using Class F Fly Ash and Elevated Temperature Curing”, *Cement and Concrete Research*, 35(6):1224-1232 (2005).
84. Palomo, A., Fernández-Jimenez, A., and Kovalchuck, G., “Some Key Factors Affecting the Alkali Activation of Fly Ash”, *2nd International Symposium of Non-Traditional Cement and Concrete*, Czech Republic, 1-12 (2005).
85. Shi, C., Krivenko, V., and Roy, M., “Alkali-Activated Cements and Concretes 1st Ed.”, *CRC Press*, London, 1-392 (2019).
86. Bakharev, T., Sanjayan, J., and Cheng, B., “Effect of Admixtures on Properties of Alkali-Activated Slag Concrete”, *Cement and Concrete Research*, 30(9):1367-1374 (2000).
87. Pacheco-Torgal, F., “1- Introduction to Handbook of Alkali-Activated Cements, Mortars and Concretes”, *Handbook of Alkali-Activated Cements, Mortars and Concretes 1st Ed.*, *Woodhead Publishing*, Portugal, 1-16 (2015).
88. Glukhovskiy, V., "Soil Silicate Articles and Structures", *Budivel'nyk Publisher*, Kiev, 1-156 (1967).
89. Krivenko, V., “Alkaline Cements”, *Proceedings of the 1st International Conference on Alkaline Cements and Concretes*, Kiev, 11-129 (1994).

90. Fernández-Jiménez, A., Puertas, F., Sobrados, I., Vesanz, J., “Structure of Calcium Silicate Hydrates Formed in Alkaline-Activated Slag: Influence of The Type of Alkaline Activator”, *Journal of The American Ceramic Society*, 86(8): 1389-1394 (2003).
91. Taylor, F., “Cement Chemistry 2nd Ed.”, *Thomas Telford*, London, (1997).
92. Duxson, P., Fernández-Jiménez, A., Provis, L., Lukey, G., Palomo, A., and Van Deventer, J., “Geopolymer Technology: The Current State of The Art”, *Journal of Materials Science*, 42(9):2917-2933 (2007).
93. Provis, J, and Van Deventer, J, “Geopolymers: Structures, Processing, Properties and Industrial Applications”, *Elsevier*, US, 1-453 (2009).
94. Duxson, P., And provis, L., “Designing Precursors for Geopolymer Cements”, *Journal of The American Ceramic Society*, 91(12):3864-3869 (2008).
95. Kirschner A., and Harmuth H., “Investigation of Geopolymerbinders With Respect to Their Application for Building Materials”, *Ceramics-Silikaty*, 48:117-120 (2004).
96. Krizan D., and Zivanovic B., “Effects of Dosage and Modulus Of water Glass on Early Hydration of Alkali-Slag Cements”, *Cement and Concrete Research*, 32:1181-1188 (2002).
97. Xiezhao, Y., “Hardening Mechanisms of An Alkaline-Activated Class F Fly Ash”, *Cement and Concrete Research*, 31:1245-1249 (2001).
98. Bakharev T., Sanjayan J., and Cheny Y-B., “Alkali-Activation of Australian Slag Cements”, *Cement and Concrete Research*, 29:113-120 (1999).
99. Xu H., and Deventer J., “The Geopolymerisation of Alumino-Silicate Minerals”, *International Journal of Mineral Processing*, 59:247-266 (2000).
100. Walling, S., Bernal, S., Gardner, L., Kinoshita, H., and Provis, J., “Blast Furnace Slag-Mg(OH)₂ Cements Activated By Sodium Carbonate”, *RSC Advances*, 8:23101-23118 (2018).
101. Matthew J., “Effect of Water-Solids Ratio on The Compressive Strength, Degree of Reaction and Microstructural Characterization of Fly Ash-Waste Glass-Based Geopolymers”, *M.Sc. Thesis, University of Minnesota, US* (2017).
102. Hardjito, D., and Rangan, V., “Development and Properties of Low-Calcium Fly Ash-Based Geopolymer Concrete” *Research Report GCI, Perth, Australia: Faculty of Engineering, Curtin University of Technology*, (2005).
103. ASTM C618-03, “Standard Specification for Coal Fly Ash and Raw or Calcined Natural Pozzolan for Use in Concrete”, *ASTM International*, West Conshohocken, PA, 2003.

104. San Nicolas, R., Walkley, B., and Van Deventer, J., “7- Fly Ash-Based Geopolymer Chemistry and Behaviour”, *Coal Combustion Products (CCP's) Characteristics, Utilization and Beneficiation*, Editors: Tom R., Anne O., and Rod J., **Woodhead Publishing**, 185-214 (2017).
105. Yang, H., Song, K., Ashour, F., and Lee, T., “Properties of Cementless Mortars Activated by Sodium Silicate”, *Construction and Building Materials*, 22:1981-1989 (2008).
106. Tillman, D., Duong, D., and Harding, N. S., “6 - Environmental Aspects of Fuel Blending”, *Solid Fuel Blending Principles, Practices, and Problems*, Editors: Tillman, D., Duong, D., and Harding, S., **Butterworth-Heinemann**, Elsevier, 249-269 (2012).
107. Fan, Y., Yin, S., Wen, Z. and Zhong, J., “Activation of Fly Ash and Its Effects on Cement Properties”, *Cement and Concrete Research*, 29(4):467-472 (1999).
108. Palomo, A., Grutzeck, W., and Blanco, T., “Alkali-Activated Fly Ashes A Cement for The Future”, *Cement and Concrete Research*, 29:1323-1329 (1999).
109. Puertas, F., Martínez-Ramírez, S., Alonso, S., and Vazquez, T., “Alkali-Activated Fly Ash/Slag Cement Strength Behaviour and Hydration Products”, *Cement and Concrete Research*, 30:1625-1632 (2000).
110. Fernandez-Jimenez, M., Palomo, A., and Lopez-Hombrados, C., “Engineering Properties of Alkali-Activated Fly Ash”, *ACI Materials Journal*, 103(2):106-112 (2006).
111. Komljenović, M., Bašćarević, Z., and Bradić, V., “Mechanical and Microstructural Properties of Alkali-Activated Fly Ash Geopolymers”, *Journal of Hazardous Materials*, 181(1-3):35-42 (2010).
112. De Vargas, S., Dal Molin, C., Vilela, C., Da Silva, J., Pavao, B., and Veit, H., “The Effects of Na₂O/SiO₂ Molar Ratio, Curing Temperature and Age on Compressive Strength, Morphology and Microstructure of Alkali-Activated Fly Ash-Based Geopolymers”, *Cement and Concrete Composites*, 33(6):653-660 (2011).
113. Micheline Moranville-Regourd, “11-Cements Made from Blast Furnace Slag”, *Lea's Chemistry of Cement and Concrete 4th Ed.*, Editors: Hewlett, P., and Liska, M., **Butterworth-Heinemann**, 637-678 (1998).
114. Grubeša, N., Barisic, I., Fucic, A., and Bansode, S., “1-Introduction”, *Characteristics and Uses of Steel Slag in Building Construction*, Editors: Grubeša, N., Barisic, I., Fucic, A., and Bansode, S., **Woodhead Publishing**, 1-14 (2016).

115. Yildirim, Z., and Prezzi, M., “Chemical, Mineralogical, and Morphological Properties of Steel Slag”, *Advances in Civil Engineering*, 1-13 (2011).
116. Wang, D., Pu, C., Scrivener, L., and Pratt, L., “Alkali-Activated Slag Cement and Concrete: A Review of Properties and Problems”, *Advances in Cement Research*, 7(27):93-102 (1995).
117. Collins, G., and Sanjayan, G., “Workability and Mechanical Properties of Alkali Activated Slag Concrete”, *Cement and Concrete Research*, 29(3): 455-458 (1999).
118. Fernández-Jiménez, A., Palomo, G., and Puertas, F., “Alkali-Activated Slag Mortars: Mechanical Strength Behaviour”, *Cement and Concrete Research*, 29(8):1313-1321 (1999).
119. Aydın, S., and Baradan, B., “Mechanical and Microstructural Properties of Heat Cured Alkali-Activated Slag Mortars”, *Materials and Design*, 35:374-383 (2012).
120. Panagiotopoulou, C., Kakali, G., Tsivilis, S., Perraki, T., and Perraki, M., “Synthesis and Characterisation of Slag Based Geopolymers”, *Materials Science Forum, Trans Tech Publications Ltd*, 636:155-160 (2010).
121. Shi, C., “Strength, Pore Structure and Permeability of Alkali-Activated Slag Mortars”, *Cement and Concrete Research*, 26(12):1789-1799 (1996).
122. Vogel, Werner, “Glass Chemistry 2nd Ed.” *Springer Science and Business Media*, US (2012).
123. Mcmillan, P.W., “Glass Ceramics 2nd Ed.”, *Academic Press*, London (1979)
124. Moncea, A. M., Badanoiu, A., Georgescu, M., and Stoleriu, S. “Cementitious Composites with Glass Waste from Recycling of Cathode Ray Tubes”, *Materials and Structures*, 46(12):2135-2144 (2013).
125. Puertas, F., And Torres-Carrasco, M., “Use of Glass Waste as An Activator in The Preparation of Alkali-Activated Slag. Mechanical Strength and Paste Characterization”, *Cement and Concrete Research*, 57:95-104 (2014).
126. Chen, T.A. “Optimum Curing Temperature and Duration of Alkali-Activated Glass Inorganic Binders”, *Journal of The Chinese Institute of Engineers*, 43(6):592-602 (2020).
127. Si, R., Guo, S., Dai, Q., and Wang, J., “Atomic-Structure, Microstructure and Mechanical Properties of Glass Powder Modified Metakaolin-Based Geopolymer”, *Construction and Building Materials*, 254(119303):1-10 (2020).

128. Dipten, M., Ms, B., Sundar, D., and Santhanam, M. "Glass Powder Based Geopolymer Binder for Precast Concrete", *International Conference on Advances in Construction Materials and Systems*, India, 3:193-201 (2017).
129. Bilondi, M. P., Toufigh, M. M., and Toufigh, V. "Experimental Investigation of Using A Recycled Glass Powder-Based Geopolymer To Improve the Mechanical Behaviour of Clay Soils", *Construction and Building Materials*, 170:302-313 (2018).
130. Si, R., Dai, Q., Guo, S., and Wang, J., "Mechanical Property, Nanopore Structure and Drying Shrinkage of Metakaolin-Based Geopolymer With Waste Glass Powder", *Journal of Cleaner Production*, 242(118502):1-12 (2020).
131. Al-Ani, T., and Sarapää, O. "Clay and Clay Mineralogy. Physical-Chemical Properties and Industrial Uses" *Geologian Tutkuskeskus*, M19/3232/2008/41: 1-91 (2008).
132. Heah, Y., Kamarudin, H., Al Bakri, M., Bnhussain, M., Luqman, M., Nizar, K., and Liew, M., "Kaolin-Based Geopolymers With Various NaOH Concentrations", *International Journal of Minerals Metallurgy and Materials*, 20:313-322 (2013).
133. Heah, Y., Kamarudin, H., Al Bakri, M., Bnhussain, M., Luqman, M., Nizar, I. K., and Liew, Y. M., "Study on Solids-To-Liquid and Alkaline Activator Ratios on Kaolin-Based Geopolymers", *Construction and Building Materials*, 35:912-922 (2012).
134. Slaty, F., Khoury, H., Wastiels, J., and Rahier, H., "Characterization of Alkali Activated Kaolinitic Clay", *Applied Clay Science*, 75-76:120-125 (2013).
135. Slaty, F., Khoury, H., Rahier, H., and Wastiels, J., "Durability of Alkali Activated Cement Produced from Kaolinitic Clay", *Applied Clay Science*, 104: 229-237 (2015).
136. Heah, Y., Kamarudin, H., Al Bakri, M., Bnhussain, M., Musa, L., Khairul Nizar, I., and Liew, Y. M., "Curing Behaviour on Kaolin-Based Geopolymers", *Advanced Materials Research*, 548:42-47 (2012).
137. Mat Daud, Y., Hussin, K., Ruzaidi, M., Osman, F., Al Bakri Abdullah, M., and Bnhussain, M., "Kaolin-Based Geopolymer Filled Epoxy-Layered Silicates: Compressive Properties", *Applied Mechanics and Materials, Trans Tech Publications Ltd.*, 754:220-224 (2015).
138. Heah, Y., Hussin, K., Al Bakri Abdullah, M., Bnhussain, M., Musa, L., Khairul Nizar, I., and Liew, M., "Strength and Microstructural Properties of Mechanically-Activated Kaolin Geopolymers", *Advanced Materials Research, Trans Tech Publications Ltd*, 626:926-930 (2013).

139. Hounsi, D., Lecomte-Nana, L., Djétéli, G., and Blanchart, P., “Kaolin-Based Geopolymers: Effect of Mechanical Activation and Curing Process”, *Construction and Building Materials*, 42:105-113 (2013).
140. Boutterin, C. and Davidovits, J. “Réticulation géopolymérique (LTGS) Et Matériaux De Construction”, *Géopolymère*, France 1:79-88 (1988).
141. Marsh, M., Andrew, H., Pascaline, P., Mark, E., and Pete, W., “Alkali Activation Behaviour of Un-Calcined Montmorillonite and Illite Clay Minerals”, *Applied Clay Science*, 166:250-261 (2018).
142. Shaqour, F., Ismeik, M., and Esaifan, M., “Alkali Activation Of Natural Clay Using A Ca(OH)₂ /Na₂CO₃ Alkaline Mixture”, *Clay Minerals*, 52:485-496 (2017).
143. Ramasamy, S., Hussin, K., Abdullah, B., Ghazali, R., Binhussain, M., and Sandu, V., “Interrelationship of Kaolin, Alkaline Liquid Ratio and Strength of Kaolin Geopolymer”, *IOP Conference Series: Materials Science and Engineering*, 133(012004):1-8 (2016).
144. Jaya, N. A., Abdullah, M. M. A. B., Ghazali, C. M. R., Hussain, M., Hussin, K., and Ahmad, R. “Kaolin Geopolymer As Precursor to Ceramic Formation”, *2nd International Conference on Green Design and Manufacture, MATEC Web of Conferences*, 78(01061):1-8 (2016).
145. Tiffo, E., Mbah, B., Belibi, B., Djobo, Y., and Elimbi, A., “Physical and Mechanical Properties of Unheated and Heated Kaolin Based-Geopolymers With Partial Replacement of Aluminium Hydroxide”, *Materials Chemistry and Physics*, 239(122103):1-10 (2020).
146. Shamala, R., Al Bakri Abdullah, M., Kamarudin, H., Yue, H., and Jin, W., “Improvement of Kaolin Based Geopolymer Coated Wood Substrates for Use in NaOH Molarity”, *Materials Science Forum, Trans Tech Publications Ltd.*, 967:241-249 (2019).
147. Heah, C., Kamarudin, H., Mohd Mustafa Al-Bakri, A., Mohamed, B., Luqman, M., Nizar, K., and Liew, M., “Effect of Alkali Concentration on Mechanical Properties of Kaolin Geopolymers”, *Romanian Journal of Materials*, 42:179-186 (2012).
148. Okoye, N., Durgaprasad, J., and Singh, B., “Fly Ash/Kaolin Based Geopolymer Green Concretes and Their Mechanical Properties”, *Data in Brief*, 5:739-744 (2015).
149. Barbosa, F., Mackenzie, J., and Thaumaturgo, C., “Synthesis and Characterisation of Materials Based on Inorganic Polymers of Alumina and Silica: Sodium Polysialate Polymers”, *International Journal of Inorganic Materials*, 2(4):309-317 (2000).

150. Davidovits J., “Chemistry of Geopolymeric Systems. Terminology”, *Proceedings of 99 Geopolymer Conference*, Saint-Quentin, France, 1:9-40 (1999).
151. Fletcher, A., Mackenzie, J., Nicholson, L., and Shimada, S., “The Composition Range of Aluminosilicate Geopolymers”, *Journal of The European Ceramic Society*, 25(9):1471-1477 (2005).
152. Davidovits J., “Geopolymer Chemistry and Sustainable Development. The Poly (Sialate) Terminology: A Very Useful and Simple Model for The Promotion and Understanding of Green-Chemistry”, In *Proceedings Of 2005 Geopolymer Conference*, Saint-Quentin, France, 1:9-15 (2005).
153. Duxson, P., Provis, L., Lukey, C., Mallicoat, W., Kriven, M., and Van Deventer, S., “Understanding the Relationship Between Geopolymer Composition, Microstructure and Mechanical Properties”, *Colloids and Surfaces A: Physicochemical and Engineering Aspects*, 269(1-3):47-58 (2005).
154. Fernández-Jiménez, A., Palomo, A., Sobrados, I., and Sanz, J. “The Role Played by The Reactive Alumina Content in The Alkaline Activation of Fly Ashes”, *Microporous and Mesoporous Materials*, 91(1-3):111-119 (2006).
155. Shi, C., Wu, X., And Tang, M., “Hydration of Alkali-Slag Cements At 150 C”, *Cement and Concrete Research*, 21(1):91-100 (1991).
156. Rahier, H., Van Mele, B., Biesemans, M., Wastiels, J., and Wu, X., “Low-Temperature Synthesized Aluminosilicate Glasses”, *Journal of Materials Science*, 31(1):71-79 (1996).
157. Van Jaarsveld, S., Van Deventer, J., and Lorenzen, L., “The Potential Use of Geopolymeric Materials to Immobilise Toxic Metals: Part I. Theory and Applications”, *Minerals Engineering*, 10(7):659-669 (1997).
158. Hos, P., McCormick, G., and Byrne, T., “Investigation of A Synthetic Aluminosilicate Inorganic Polymer”, *Journal of Materials Science*, 37(11): 2311-2316 (2002).
159. Bakharev, T., Sanjayan, J., and Cheny, Y-B., “Alkali-Activation of Australian Slag Cements”, *Cement and Concrete Researches*, 29:113-120 (1999).
160. Pinto AT., “Alkali-Activated Metakaolin Based Binders”, *Ph.D. Thesis, University of Minho*, Portugal, (2004).
161. Wang H., Li H., and Yan F., “Synthesis and Mechanical Properties of Metakaolinite-Based Geopolymer”, *Colloids Surf*, 268:1-6 (2005).
162. Cercel, J., Adesina, A., and Das, S., “Performance of Eco-Friendly Mortars Made with Alkali-Activated Slag and Glass Powder as A Binder”, *Construction and Building Materials*, 121457:1-13 (2020).

163. Özkan, Ö., and Yüksel, İ., “Studies on Mortars Containing Waste Bottle Glass and Industrial By-Products”, *Construction and Building Materials*, 22(6): 1288-1298 (2008).
164. Chen, T., “Effects of Aging and Curing Processes on The Property of Alkali-Activated Glass Inorganic Binders.” *Ph.D. Thesis, National Cheng Kung University*, Taiwan, (2016).
165. Cyr, M., Idir, R., and Poinot, T., “Properties of Inorganic Polymer (Geopolymer) Mortars Made of Glass Cullet”, *Journal of Materials Science*, 47(6):2782-2797 (2012).
166. Rivera, F., Cuarán-Cuarán, I., Vanegas-Bonilla, N., and De Gutiérrez, M., “Novel Use of Waste Glass Powder: Production of Geopolymeric Tiles”, *Advanced Powder Technology*, 29(12):3448-3454 (2018).
167. Novais, M., Ascensão, G., Seabra, P., and Labrincha A., “Waste Glass from End-Of-Life Fluorescent Lamps as Raw Material in Geopolymers”, *Waste Management*, 52:245-255 (2016).
168. He, J., “Synthesis and Characterization of Geopolymers For Infrastructural applications”, *Ph.D. Thesis, The Graduate Faculty of The Louisiana State university and Agricultural and Mechanical College*, U.S, (2012).
169. Chindaprasirt, P., Jaturapitakkul, C., Chalee, W., Rattanasak, U., “Comparative Study on The Characteristics of Fly Ash and Bottom Ash Geopolymers”, *Waste Manage*, 29:539-543 (2009).
170. Redden, R., and Neithalath, N., “Microstructure, Strength, and Moisture Stability of Alkali Activated Glass Powder-Based Binders”, *Cement and Concrete Composites*, 45:46-56 (2014).
171. Yip, K., and Van Deventer, J., “Microanalysis of Calcium Silicate Hydrate Gel Formed Within a Geopolymeric Binder”, *Journal of Materials Science*, 38(18):3851-3860 (2003).
172. Campbell, H., and Folk, L., “Ancient Egyptian Pyramids-Concrete or Rock”, *Concrete International*, 13(8):28-30 (1991).
173. Marsh, A., Heath, A., Patureau, P., Evernden, M., and Walker, P. “Stabilisation of Clay Mixtures and Soils by Alkali Activation”, *Earthen Dwellings and Structures*, Singapore, 15-26 (2019).
174. Provis, L., Yong, Z., Duxson, P., and Van Deventer, S., “Correlating Mechanical and Thermal Properties of Sodium Silicate-Fly Ash Geopolymers”, *Colloids and Surfaces A: Physicochemical and Engineering Aspects*, 336(1-3):57-63 (2009).

175. Zuhua, Z., Xiao, Y., Huajun, Z., and Yue, C. "Role of Water in The Synthesis of Calcined Kaolin Based Geopolymer", *Applied Clay Science*, 43(2):218-223 (2009).
176. Prasad, S., Reid, J., and Murray, H., "Kaolin: Processing, Properties and Applications", *Applied Clay Science*, 6(2):87-119 (1991).
177. Heah, C., Kamarudin, H., Mustafa Al Bakri, A., Bnhussain, M., Luqman, M., Khairul Nizar, I., Ruzaidi, M., and Liew, Y., "Optimization of Solids-To-Liquid and Alkali Activator Ratios of Calcined Kaolin Geopolymeric Powder", *Construction and Building Materials*, 37:440-451 (2012).
178. De Silva, P., Sagoe-Crenstil, K., and Sirivivatnanon, V., "Kinetics of Geopolymerization: Role of Al₂O₃ and SiO₂", *Cement and Concrete Research*, 37(4): 512-518 (2007).
179. Rowles, M., O'Connor, B., "Chemical Optimisation of The Compressive Strength of Aluminosilicate Geopolymers Synthesised by Sodium Silicate Activation of Metakaolinite", *Journal of Materials Chemistry*, 13(5):1161-1165 (2003).
180. Zhang, B., Mackenzie, J., and Brown, W., "Crystalline Phase Formation in Metakaolinite Geopolymers Activated with NaOH and Sodium Silicate", *Journal of Materials Science*, 44(17):4668-4676 (2009).
181. Provis, L., Yong, L., and Duxson, P., "5-Nanostructure/Microstructure of Metakaolin Geopolymers", *Geopolymers*, Woodhead Publishing, 72-88 (2009).
182. Wang, D., and Scrivener, L., "Hydration Products of Alkali Activated Slag Cement", *Cement and Concrete Research*, 25(3):561-571 (1995).
183. Zhihua P., Dongxu L., Jian Y., and Nanry Y., "Hydration Products of Alkali-Activated Slag Red Mud Cementitious Material", *Cement Concrete Research*, 32:357-362 (2002).
184. Zhihua P., Dongxu L., Jian Y., and Nanry Y., "Properties and Microstructure of The Hardened Alkali-Activated Red Mud-Slag Cementitious Material", *Cement and Concrete Research*, 32(3):357-362 (2002).
185. Brough, R., and Atkinson, A. "Sodium Silicate-Based, Alkali-Activated Slag Mortars: Part I. Strength, Hydration and Microstructure", *Cement and Concrete Research*, 32(6):865-879 (2002).
186. Song, S., Sohn, D., Jennings, M., and Mason, O. "Hydration of Alkali-Activated Ground Granulated Blast Furnace Slag", *Journal of Materials Science*, 35(1):249-257 (2000).
187. Puertas, F., Fernández-Jiménez, A., and Blanco-Varela, M. T. "Pore Solution in Alkali-Activated Slag Cement Pastes. Relation to The Composition and

- Structure of Calcium Silicate Hydrate”, *Cement and Concrete Research*, 34(1):139-148 (2004).
188. Xiao, R., Polaczyk, P., Zhang, M., Jiang, X., Zhang, Y., Huang, B., and Hu, W. “Evaluation of Glass Powder-Based Geopolymer Stabilized Road Bases Containing Recycled Waste Glass Aggregate”, *Transportation Research Record*, 2674(1):22-32 (2020).
 189. Torres-Carrasco, M., and Puertas, F. “Waste Glass as A Precursor in Alkaline Activation: Chemical Process and Hydration Products”, *Construction and Building Materials*, 139:342-354 (2017).
 190. Van Jaarsveld, S., Van Deventer, J., and Lukey, C., “The Effect of Composition and Temperature on The Properties of Fly Ash- and Kaolinite-Based Geopolymers”, *Chemical Engineering Journal*, 89(1-3):63-73 (2002).
 191. Pnias, D., Giannopoulou, P., and Perraki, T., “Effect of Synthesis Parameters on The Mechanical Properties of Fly Ash-Based Geopolymers”, *Colloids and Surfaces A: Physicochemical and Engineering Aspects*, 301(1-3):246-254 (2007).
 192. Galan, E., Aparicio, P., Miras, A., Michailidis, K., and Tsirambides, A., “Technical Properties of Compounded Kaolin Sample from Griva (Macedonia, Greece)”, *Applied Clay Science*, 10(6):477-490 (1996).
 193. Djobo, Y., Tchadjié, N., Tchakoute, K., Kenne, D., Elimbi, A., and Njopwouo, D., “Synthesis of Geopolymer Composites from A Mixture of Volcanic Scoria and Metakaolin”, *Journal of Asian Ceramic Societies*, 2(4):387-398 (2014).
 194. Van Der Marel, W., and Beutelspacher, H., “Atlas of Infrared Spectroscopy of Clay Minerals and Their Admixtures”, *Elsevier Publishing Company*, Amsterdam, 1-396 (1976).
 195. Granizo, L., Blanco-Varela, T., and Martínez-Ramírez, S., “Alkali Activation of Metakaolins: Parameters Affecting Mechanical, Structural and Microstructural Properties”, *Journal of Materials Science*, 42(9):2934-2943 (2007).
 196. De Benedetto, E., Laviano, R., Sabbatini, L., and Zambonin, G., “Infrared Spectroscopy in The Mineralogical Characterization of Ancient Pottery”, *Journal of Cultural Heritage*, 3(3):177-186 (2002).
 197. Bich, C., Ambroise, J., and Péra, J. “Influence of Degree of Dehydroxylation On the Pozzolanic Activity of Metakaolin”, *Applied Clay Science*, 44(3-4): 194-200 (2009).
 198. Cheng, H., Yang, J., Liu, Q., Zhang, J., and Frost, R. L., “A Spectroscopic Comparison of Selected Chinese Kaolinite, Coal Bearing Kaolinite and Halloysite-A Mid-Infrared and Near-Infrared Study”, *Spectrochimica Acta Part A: Molecular and Biomolecular Spectroscopy*, 77(4):856-861 (2010).

199. Madejova, J., and Komadel, P., "Baseline Studies of The Clay Minerals Society Source Clays: Infrared Methods", *Clays and Clay Minerals*, 49(5): 410-432 (2001).
200. Russell, D., and Fraser, R., "Infrared Methods", *Clay Mineralogy: Spectroscopic and Chemical Determinative Methods*, **Springer**, Dordrecht, 11-67 (1994).
201. Russel, D., "Infrared Spectroscopy of Inorganic Compounds", *Laboratory Methods in Infrared Spectroscopy*, **Wiley**, New York, (1987).
202. Henderson, B., and Taylor, D. "Infrared Spectra of Anhydrous Members of The Sodalite Family", *Spectrochimica Acta Part A: Molecular Spectroscopy*, 33(3-4):283-290 (1977).
203. Mikuła, A., Król, M., and Koleżyński, A., "The Influence of The Long-Range Order on The Vibrational Spectra of Structures Based on Sodalite Cage", *Spectrochimica Acta Part A: Molecular and Biomolecular Spectroscopy*, 144:273-280 (2015).
204. Elimbi, A., Tchakoute, K., Kondoh, M., and Manga, D. "Thermal Behaviour and Characteristics of Fired Geopolymers Produced from Local Cameroonian Metakaolin", *Ceramics International*, 40(3):4515-4520 (2014).
205. Abbas, R., Khereby, A., Ghorab, Y., and Elkhoshkhany, N. "Preparation of Geopolymer Concrete Using Egyptian Kaolin Clay and The Study of Its Environmental Effects and Economic Cost", *Clean Technologies and Environmenta Policy*, 22(4):1-19 (2020).
206. Engelhardt, G., Felsche, J., and Sieger, P. "The hydrosodalite system $\text{Na}_{6+x}[\text{SiAlO}_4]_6(\text{OH})_x \cdot n\text{H}_2\text{O}$: formation, phase composition, and de- and rehydration studied by ^1H , ^{23}Na , and ^{29}Si MAS-NMR spectroscopy in tandem with thermal analysis, x-ray diffraction, and IR spectroscopy", *Journal of the American Chemical Society*, 114(4): 1173-1182 (1992).

RESUME

Zaid Kareem is an engineer, he enrolled in bachelor program in engineering faculty at Al-Mustansiriya University / Iraq, then, he graduated in 2013. Zaid worked as an engineer in many constructional and energy projects, and he worked as a lecturer in a number of Iraqi universities until the beginning of 2019, as he enrolled in the master's program at Karabük University / Turkey.